I⋆M⋆P⋆R⋆S on ASTROPHYSICS at LMU Munich

Astrophysics Introductory Course

Lecture given by

Ralf Bender

in collaboration with:

Chris Botzler, Andre Crusius-Wätzel,
Niv Drory, Georg Feulner, Armin Gabasch,
Ulrich Hopp, Claudia Maraston,
Michael Matthias, Jan Snigula, Daniel Thomas

Fall 2001

Chapter 2

The Stars:
Spectra and Fundamental Properties

2.1 Magnitudes and all that ...

The **apparent magnitude** m at frequency ν of an astronomical object is defined via:

$$m_\nu \;=\; -2.5 \log \left[\frac{f_\nu}{f_\nu(Vega)} \right]$$

with f_ν being the object's flux (units of W/m^2/Hz). In this **classical or Vega magnitude system** Vega (α Lyrae), an A0V star (see below), is used as the reference star. In the Vega magnitude system, Vega has magnitude 0 at all frequencies.

The logarithmic magnitude scale mimicks the intensity sensitivity of the human eye. It is defined in a way that it roughly reproduces the ancient Greek magnitude scale (0...6 = brightest... faintest stars visible by naked eye).

Today, the **AB-magnitude system** is becoming increasingly popular. In the AB-system a source of constant f_ν has constant magnitude:

$$m_{AB} \;=\; -2.5 \log \left[\frac{f_\nu}{(3.6308 \times 10^{-23} W/Hz/m^2)} \right]$$

The normalizing flux is chosen in a such a way that Vega magnitudes and AB-magnitudes are the same at 5500Å.

In most observations, the fluxes measured are not monochromatic but are integrated over a *filter bandpass*. Typical **broad band filters** have widths of several hundred to 2000Å.

The magnitude for a filter x ($T_x(\nu) =$transmission function) is then defined via:

$$m_x = -2.5 \log \left[\frac{\int f_\nu T_x(\nu) d\nu}{\int f_{\nu,Vega} T_x(\nu) d\nu} \right]$$

Several filter systems were designed:

- Johnson UBVRIJHKLMN
- Kron-Cousins $R_C I_C$
- Stroemgrenu v b y Hβ
- Gunn ugriz
- Sloan Digitial Sky Survey filters: u′ g′ r′ i′ z′ , probably the standard of the future

whereby U = near UV, B = blue, V = visual(green), R = red, I = near infrared, JHKLMN = infrared

A typical precision which can be obtained relatively easily is: $\Delta m \sim \Delta f_x / f_x \sim 0.02$.

Absolute radiation fluxes S_λ for an A0V star with visible brightness V = 0 mag (and because it is an A0V star like Vega, it obviously has UBVRIJHKLMN = 0 in the Vega magnitude system) for the effective wavelengths of the Johnson filters

Filter	$\lambda[\mu\text{m}]$	$S_\lambda[\text{Wm}^{-2}\text{nm}^{-1}]$
U	0.36	3.98×10^{-11}
B	0.44	6.95×10^{-11}
V	0.55	3.63×10^{-11}
R	0.70	1.70×10^{-11}
I	0.90	8.29×10^{-12}
J	1.25	3.03×10^{-12}
K	2.22	3.84×10^{-13}
L	3.60	6.34×10^{-14}
M	5.00	1.87×10^{-14}
N	10.60	1.03×10^{-15}

The value given for V corresponds to
$S_V = 3.66 \times 10^{-23}\text{Wm}^{-2}\text{Hz}^{-1}$
$N = 1004$ photons $\text{cm}^{-2}\text{Å}^{-1}$

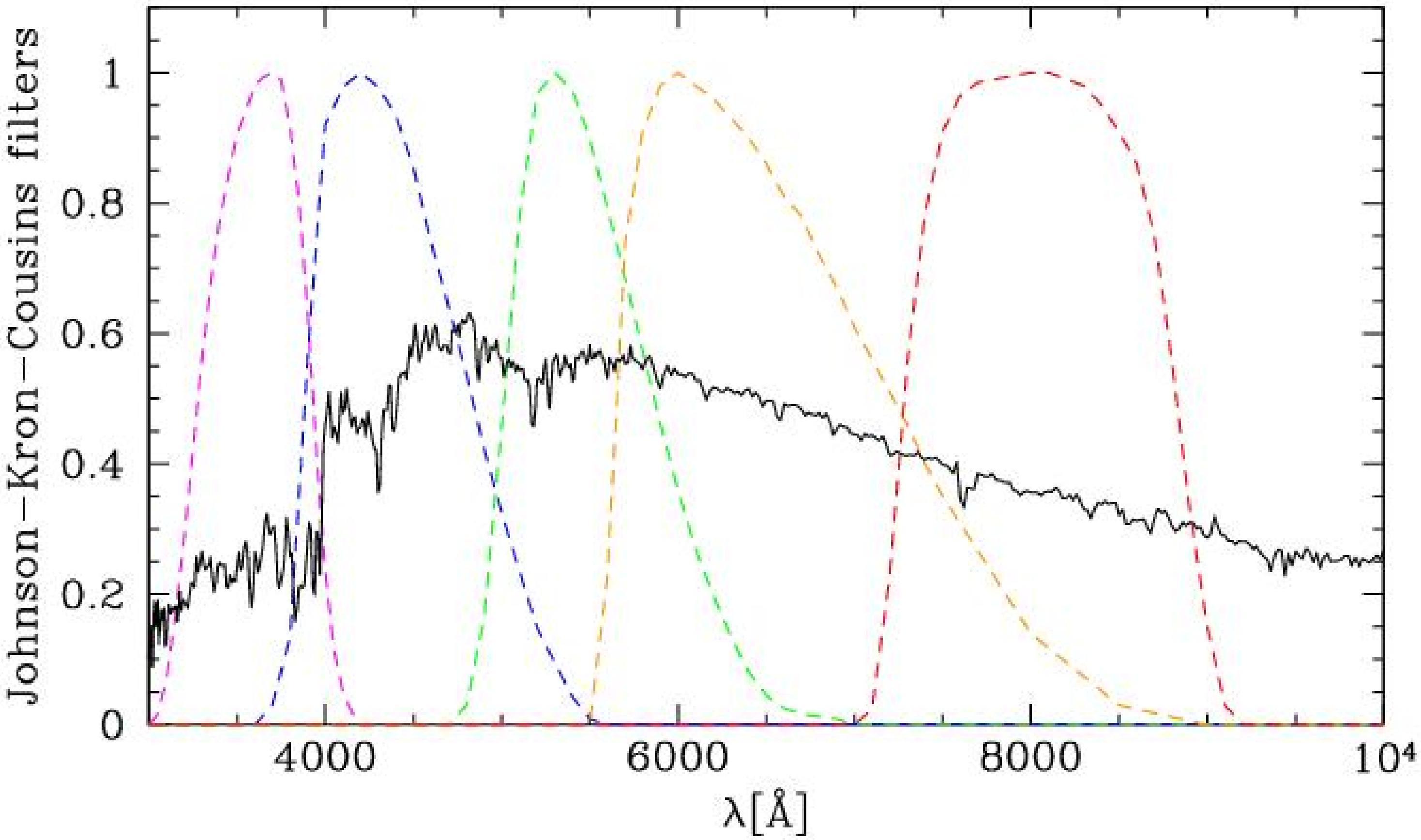

Transmission curves for the currently most widely used Johnson UBV, Kron Cousins RI filter system, as reconstructed by Bessel (PASP, 1990). A G5V star (similar to the sun, but somewhat cooler) is overplotted for comparison.

Colors or **color indices** of objects are defined as differences between filter magnitudes in different bands:

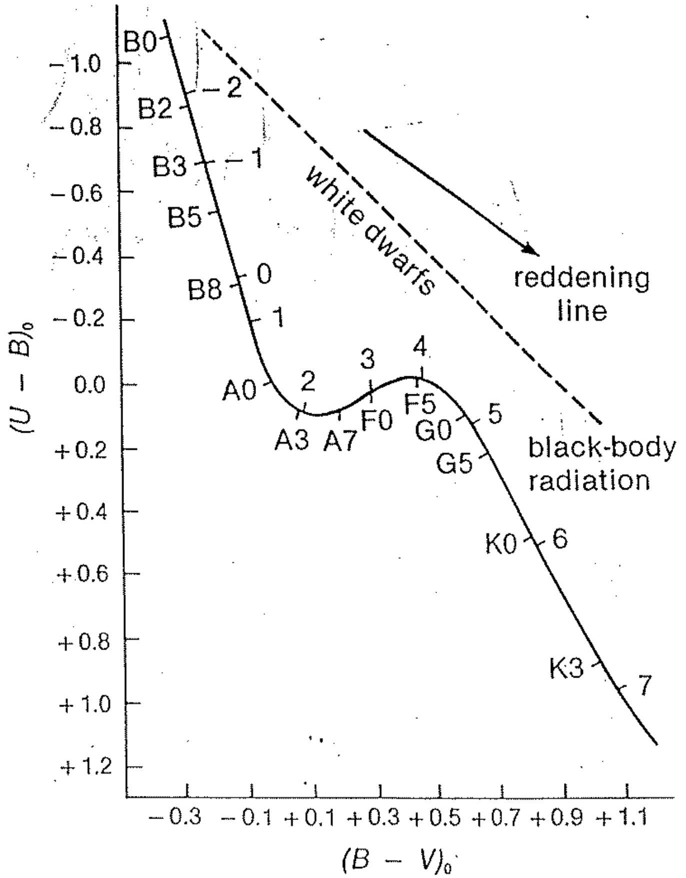

U-B = $m_U - m_B$
B-V = $m_B - m_V$
...

- The left diagram shows the distribution of stars in the $U-B$ vs $B-V$ plane, stellar types O,B,A,... are explained below.
- large numerical values of the index indicate red objects, small values blue objects.
- the arrow indicates the effect of reddening by interstellar dust

Absolute magnitudes are introduced as a measure of the intrisic (distance independent) luminosity:

$$\mathbf{M} = \mathbf{m} - \mathbf{5}\log\left(\frac{\mathbf{D}}{\mathbf{10pc}}\right)$$

with:
M = the absolute magnitude
m = the apparent magnitude
D = the distance measured in parsec (1pc = 3.2616 light years$= 3.0856 \times 10^{18}$ cm)
m - M is called the **distance modulus**

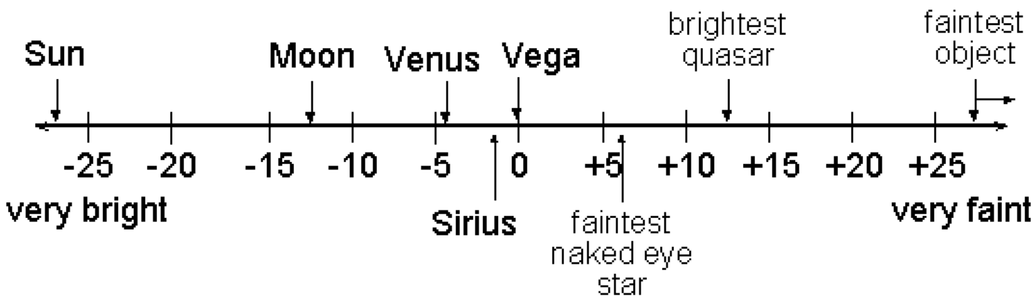

Apparent brightnesses of some objects in the magnitude system.

Note: parsecs are the standard distance unit in astrophysics. Parsec means parallax second. The radius of the earth orbit, seen from a distance of 1 pc corresponds to an angular distance of 1 arcsec.

Bolometric magnitudes m_{bol} are a measure for the total luminosity integrated over all wavelengths. One defines:

$$m_{bol} = m_V + \text{B.C.}$$

where B.C. is called bolometric correction and defined in such a way that for almost all stars B.C.> 0. B.C. ~ 0 for F to G stars (because these have their emission maximum in the V-band). Bolometric magnitudes are generally not used for objects other than stars.

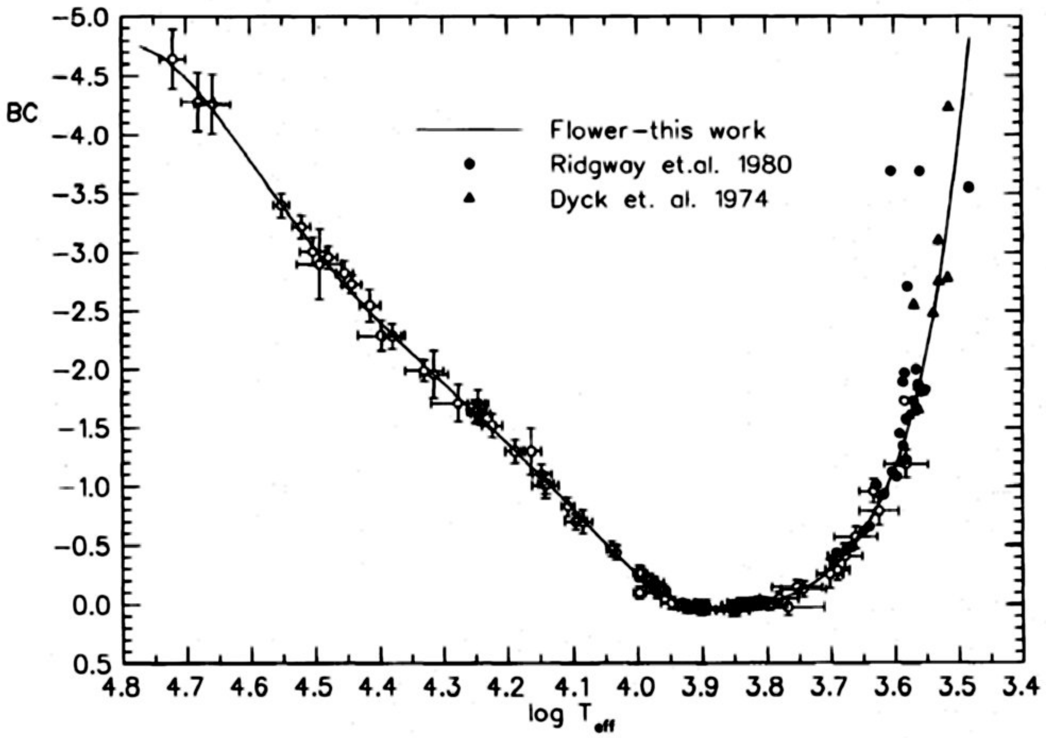

Bolometric correction as a function of effective temperature T_{eff} from Flower, 1996, ApJ

Transformation of absolute magnitudes into luminosities in solar units $L/L_\odot$:

$$M_V - M_{V,\odot} = -2.5 \log \frac{L_V}{L_{V,\odot}}$$

The absolute magnitude of the sun is: $M_{B,\odot} = 5.48,\ M_{V,\odot} = 4.83,\ M_{K,\odot} = 3.33$ ...
(see Cox et al: Aller's Astrophysical Quantities)

Absorption and Extinction

The flux of an astronomical object measured on earth needs to be corrected for two effects (at least):

- Absorption in the atmosphere of the earth. If $m_{\lambda,obs}$ is the magnitude of a object measured at a zenith distance angle θ and ϵ_λ is the absorption of the atmosphere in the zenith, then we obtain the magnitude of the object outside the atmosphere $m_{\lambda,corr}$ via:

$$m_{\lambda,corr} = m_{\lambda,obs} - \epsilon_\lambda / cos(\theta)$$

(valid for angles below 70 degrees, assuming a plane-parallel atmosphere). Typical values for ϵ_λ in the optical decrease from 0.3 around 4000Å to 0.1 around 8000Å (exact values have to be derived from the observations of standard stars).

- Extinction and absorption by dust grains and gas between the object and the earth. The extinction is largely proportional to the column density of the interstellar gas between us and the object. For distant stars and extragalactic objects, the so-called *Galactic infrared cirrus* is a good indicator of extinction as it is produced by the thermal emission of the dust in the MIlky Way. The extinction is maximal in the galactic plane, and minimal perpendicular to it.

  The interstellar extinction reddens an object which is described by the *colour excess*:

$$E_{B-V} = (B-V)_{obs} - (B-V)_o$$

  The extinction is, e.g., given for the V-filter via:

$$m_{V,obs} = m_{V,o} + A_V$$

  In these equations “obs” denotes observed values (with extinction), “o” denotes intrinsic ones. The relation between A_V and E_{B-V} is:

$$A_V = 3.1 E_{B-V}$$

  The ‘Galactic absorption law’ relating A_V to A_λ can be read from the diagram on the next page.

  The extinction to star clusters can be determined, e.g., from a 2-colour-diagram, (especially the U-V vs B-V diagram where the reddening vector is slightly shallower than the black-body line).

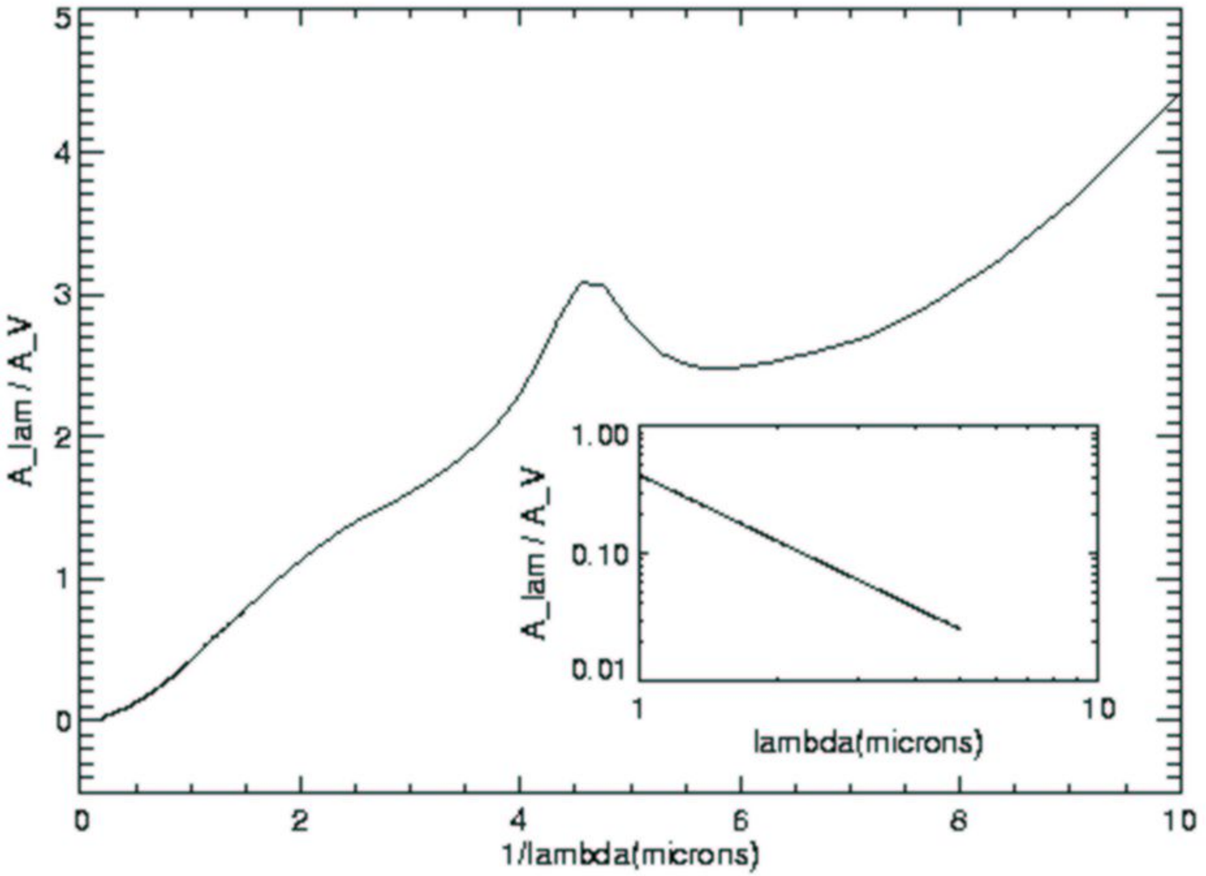

Averaged interstellar extinction curve A_λ according to Savage&Mathis (1979).

2.2 Stellar Spectra

Spectra of stars contain a wealth of detailed information about the properties of stars. Surface temperatures, masses, radii, luminosities, chemical compositions etc can be derived from the analysis of stellar spectra. Some historical milestones:

- Wollaston was probably the first who reported a few dark lines in the solar spectrum in 1802. However his equipment was poor and he failed to recognize the importance of this observation. The real starting point of solar (and stellar) spectroscopy were Fraunhofers pioneering studies in 1816-1820 in Benediktbeuren and in the Munich Observatory together with von Soldner. Fraunhofer discovered numerous absorption lines in the solar spectrum and documented them with impressing accuracy. The first (hand-drawn) stellar spectra were recorded by Lamont in the 1830s, also in Munich-Bogenhausen.
- The physical and chemical analysis of stars began with Kirchoff and Bunsen in Heidelberg who identified Fraunhofers D-lines in the sun and in other stars as absorption lines of sodium (1859). They also discovered the previously unknown elements caesium and rubidium.
- Doppler predicts the ‘Doppler’-effect in 1842. Scheiner in Potsdam and Keeler at Lick Observatory verified his prediction around 1890.

- The spectral classification was started by Secchi and Vogel and improved by Draper around 1880. Under surveillance of Annie Jump Cannon the extended Henry-Draper catalog with 200.000 stars is compiled from 1918–1924 using objectiv prism plates.

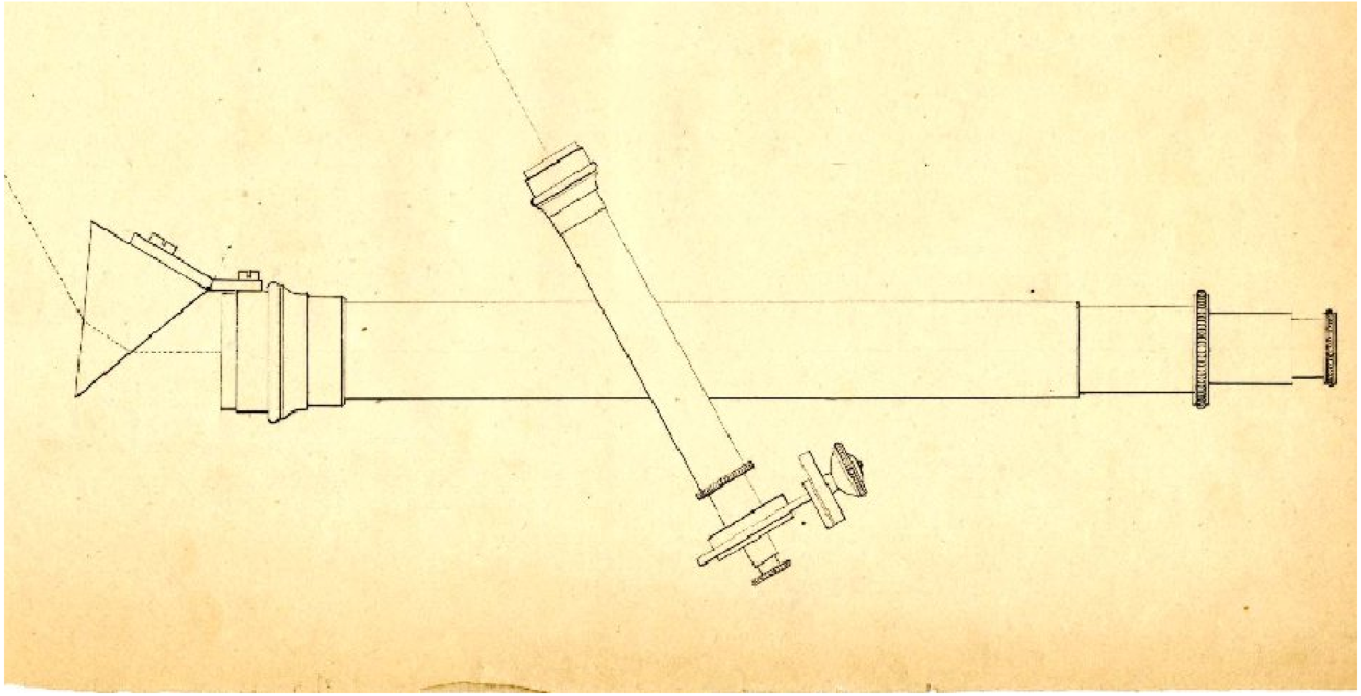

Fraunhofer’s telescope with the first objective prism (around 1816). With this instrument he observed stellar spectra together with von Soldner.

2.2.1 Harvard classification (extended by L and T types).

```
                                       S
                                      /
O  -  B  -  A  -  F  -  G  - K  -  M  -  L  -  T
                         \
                          R - N
```

colour:	blue	white	yellow	red	infrared
B - V :	-0.3	0.0	0.4	0.8	1.5

The Harvard classification is a sequence in color, effective temperature T_{eff} and varying strengths of absorption lines.

A fine division is given by the digits 0-9 : B0, B1, ..., B9

The letters have no meaning but there exist funny (or stupid?) sentences to memorize the main types, like:

Oh Be A Fine Girl, Kiss Me Right Now (american style), or

Ohne Bier Aus'm Fass Gibt's Koa Mass (bavarian style) ...

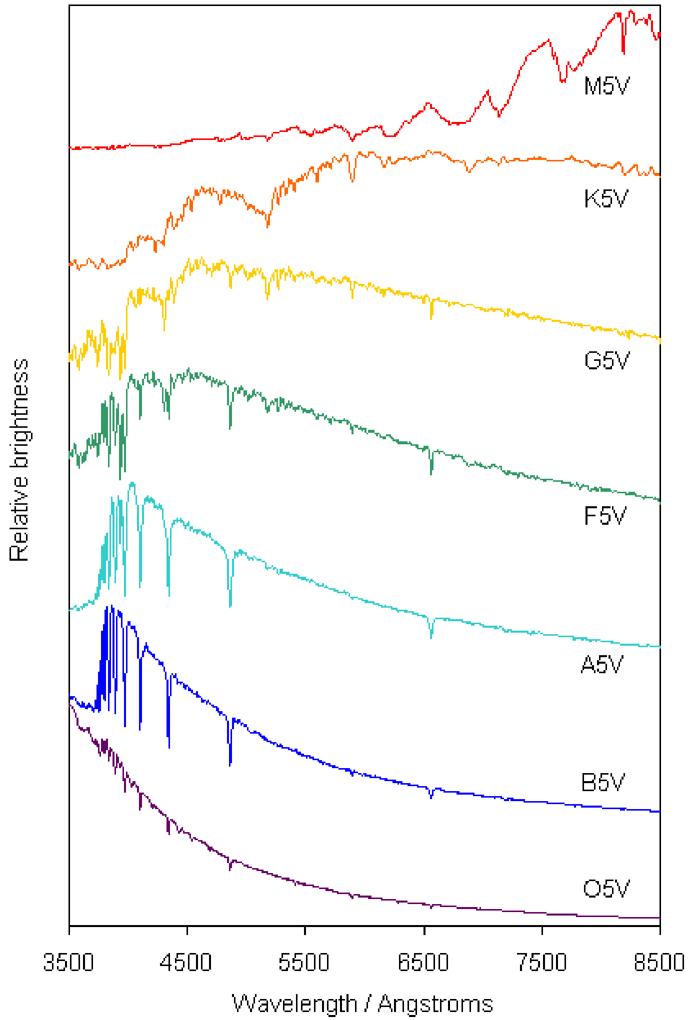

Spectral intensity distributions of stars of different Harvard type.

Tabelle I.11: Mittlere Farbindizes und bolometrische Korrektion *B. C.* verschiedener Spektraltypen (Leuchtkraftklasse V, vgl. I.2.9)

Sp	$(U-V)_0$	$(B-V)_0$	$(V-R)_0$	$(V-I)_0$	$(V-J)_0$	$(V-K)_0$	$(V-L)_0$	*B. C.*
O5–7	−1.46	−0.32	−0.15	−0.47	−0.73	−0.94	−1.01	−3.73
B0	−1.38	−0.30	−0.13	−0.42	−0.70	−0.93	−0.99	−2.96
B5	−0.72	−0.16	−0.06	−0.22	−0.35	−0.47	−0.48	−1.26
A0	0.00	0.00	0.00	0.00	0.0	0.00	0.00	−0.10
A5	+0.25	+0.14	+0.16	+0.22	+0.27	+0.36	+0.40	+0.05
F0	0.37	0.31	0.30	0.47	0.58	0.79	0.86	+0.11
F5	0.43	0.43	0.40	0.64	0.79	1.07	1.25	+0.06
G0	0.70	0.59	0.50	0.81	1.03	1.35	1.53	+0.02
G5	0.86	0.66	0.54	0.89	1.14	1.49	1.67	−0.01
K0	1.29	0.82	0.64	1.06	1.38	1.83	2.00	−0.11
K5	2.18	1.15	0.99	1.62	2.04	2.75	2.84	−0.52
M0	2.67	1.41	1.28	2.19	2.71	3.60	3.78	−1.18
M5	2.80	1.61	1.80	3.47	4.28	5.17	(5.54)	−2.53

from Scheffler and Elsässer: The physics of the sun and the stars, Springer Verlag

2.2.2 Temperatures of stars

To first order, the spectral energy distributions of stars can be described by a black-body spectrum (Planck's radiation law; units: ergs/cm^2/s/Å):

$$\mathbf{B_\lambda(T) = \frac{2hc^2}{\lambda^5}\frac{1}{e^{hc/\lambda k_B T} - 1}}$$

The maximum energy is emitted at a wavelength defined by Wien's Displacement law:

$$\lambda_{\max} = \frac{\mathbf{3 \times 10^7}\text{Å}}{\mathbf{T/k_B}}$$

while the integral over wavelength gives the Stefan-Boltzmann law:

$$\mathbf{B(T) = \int d\lambda\, B_\lambda(T) = \sigma T^4}$$

This allows to assign stars of different type an **effective temperature** T_{eff} which is related to luminosity L and radius R of the star:

$$L \;=\; 4\pi R^2 \sigma T_{eff}^4$$

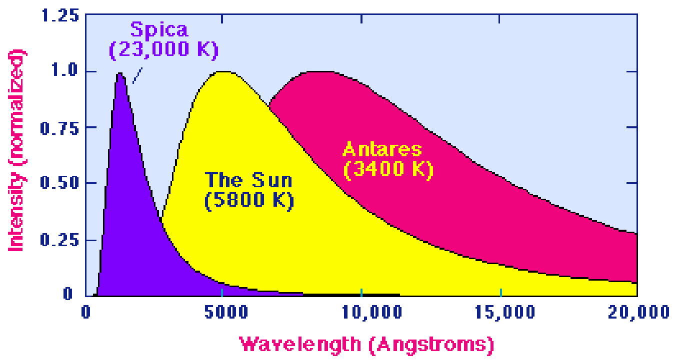

.

1996ApJ...469..355

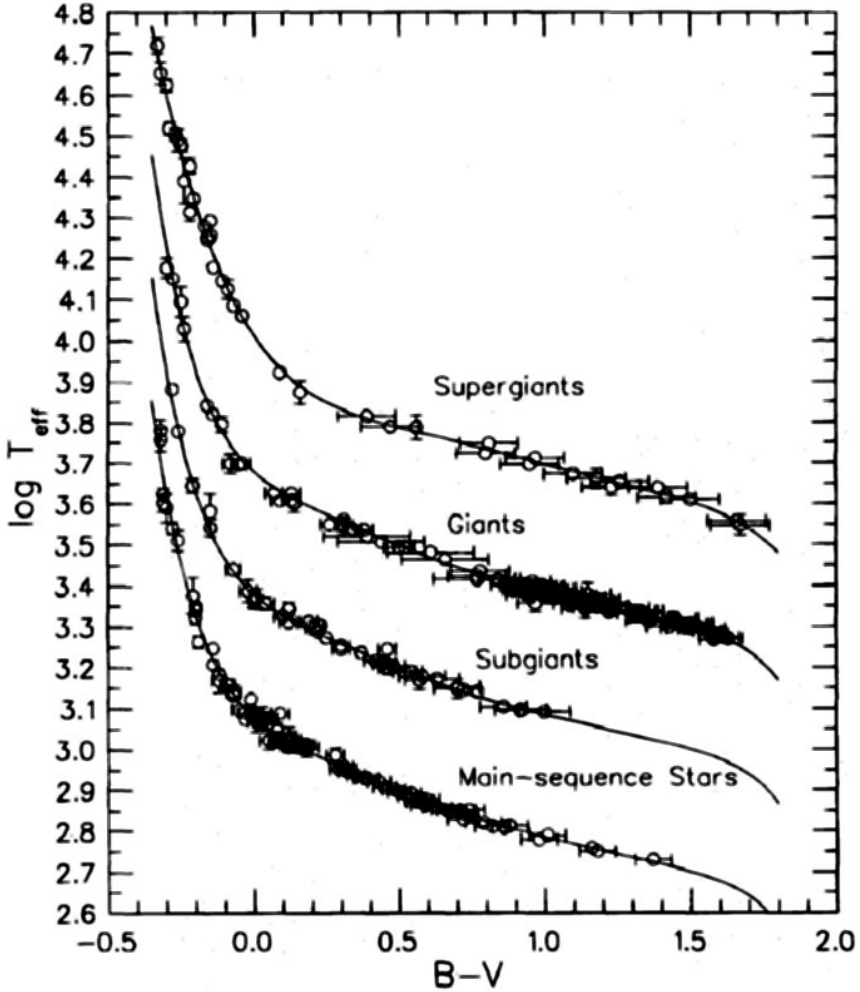

FIG. 5.—Polynomial fits to temperatures and colors. Temperatures of giants, subgiants, and main-sequence stars are lower by 0.3 in log T_{eff} than the next more luminous class. The lower three curves are identical; the curve is the polynomial fit to all giants, subgiants, and main-sequence stars in the database listed in Table 5 (except those of Ridgway et al. 1980). Symbols for stars without error bars are larger than the error bars.

Relation between B-V color and effective temperature T_{eff} from Flower, 1996, ApJ.

The different types of stars (see below) are offset from each other by 0.3 dex.

2.2.3 Continuum shape and absorption lines in stellar spectra

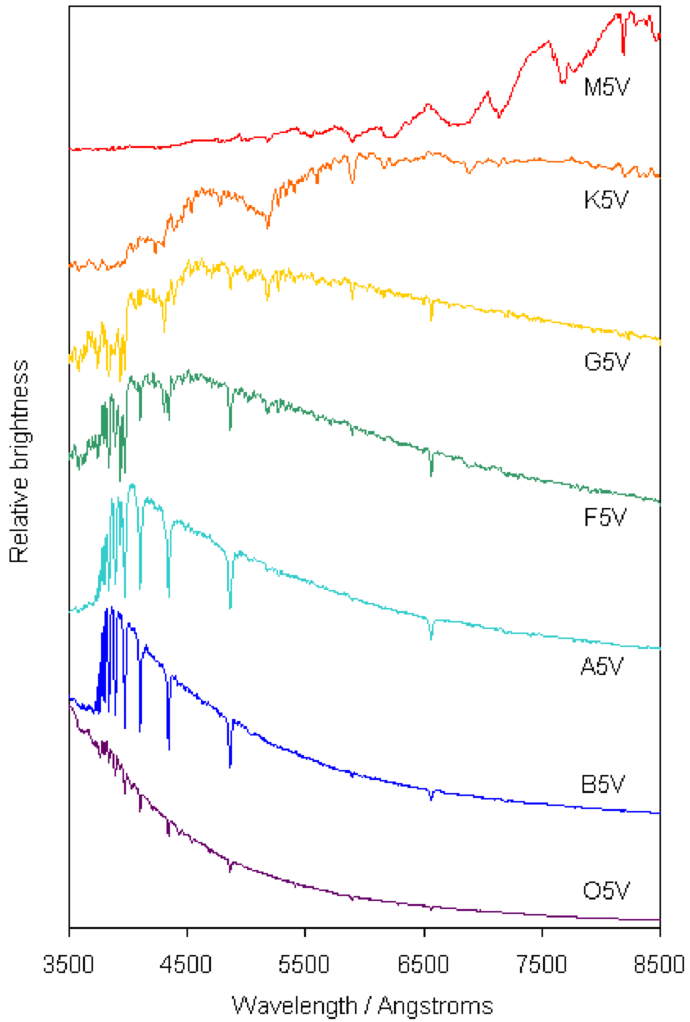

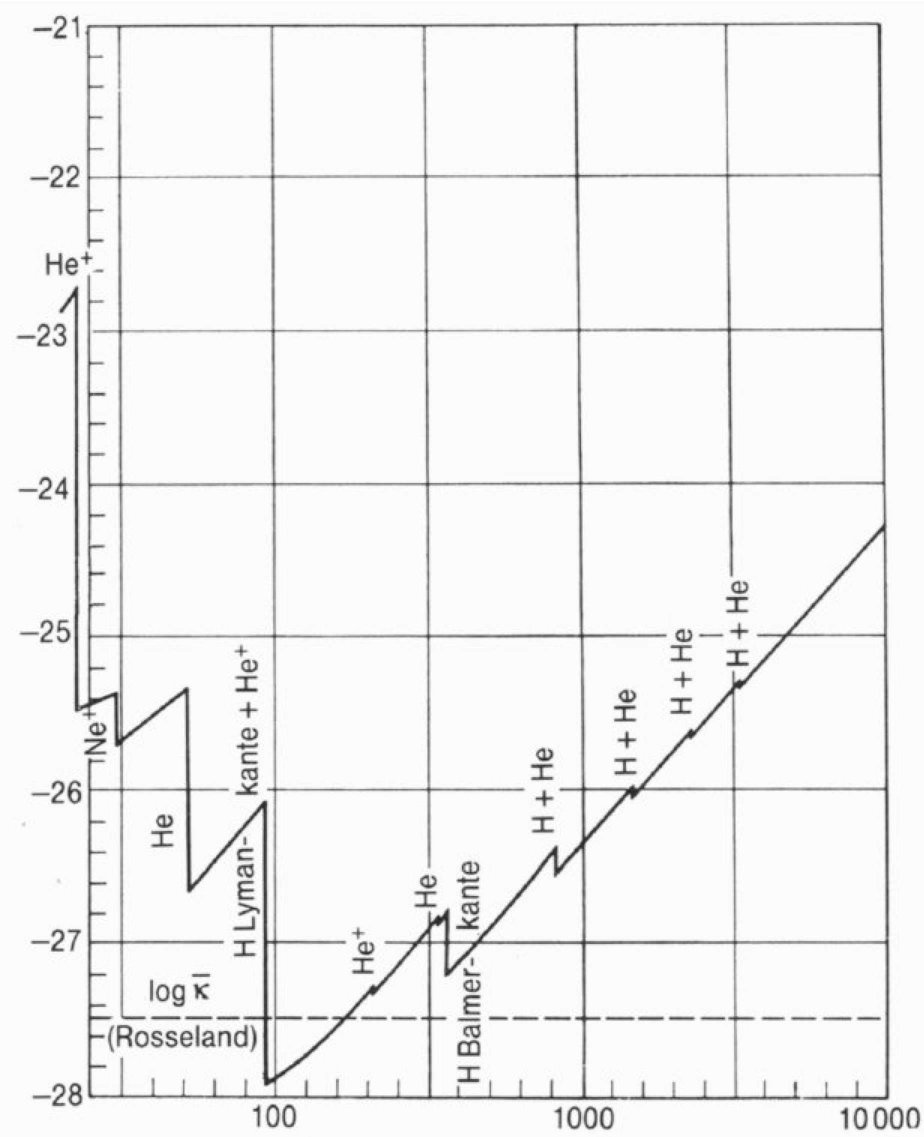

κ/ρ (in m^2/nucleon) against λ in nm for τ Sco ($T = 28000$K). The wavelength dependence of κ provides a first order explanation for the energy distribution of stellar spectra. Assume for simplicity that a stellar atmosphere is mostly a cool, optically thin gas layer above a hotter black-body emitting stellar interior of temperature T_i. Then, the spectrum we are expecting to see is a black body $B_\nu(T_i)$, modified by the extinction κ_ν of the atmosphere, i.e.

$$I_\nu = B_\nu(T_i) \cdot (1 - \kappa_\nu s)$$

where s is the thickness of the atmosphere. Compare the shape of this κ curve with the spectral shape of the B5 star two pages ago. The Balmer break ('Balmer-Kante') can be explained by the κ function.

Solar Absorption Spectrum

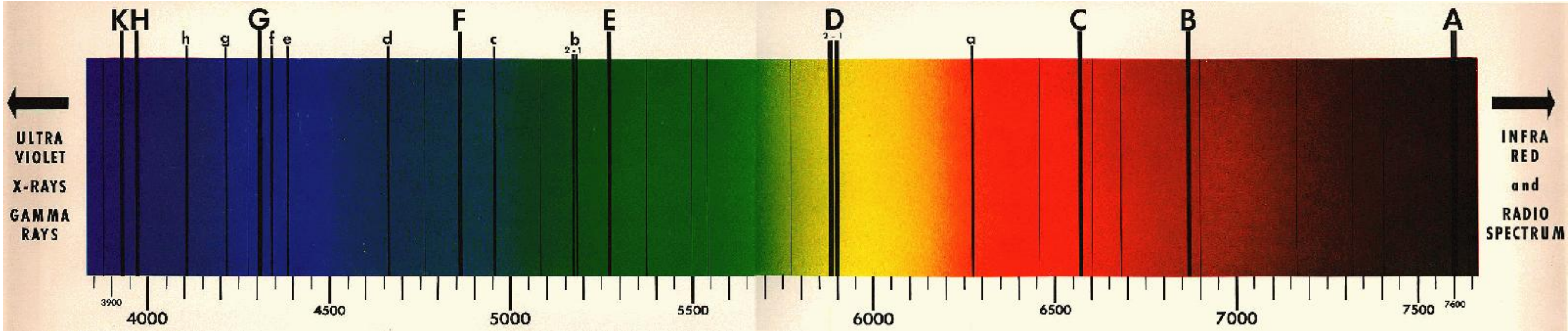

The following elements give rise to these lines:

- Hydrogen H (C; F; f; h)
- Sodium Na (D–1,2)
- Magnesium Mg (b–1,2)
- Calcium Ca (G; g; H; K)
- Iron Fe (E; c; d; e; G)
- Oxygen O_2 (telluric: A–, B–band; a–band)

Variation of absorption lines along the Harvard sequence, i.e. as a function of T_{eff}

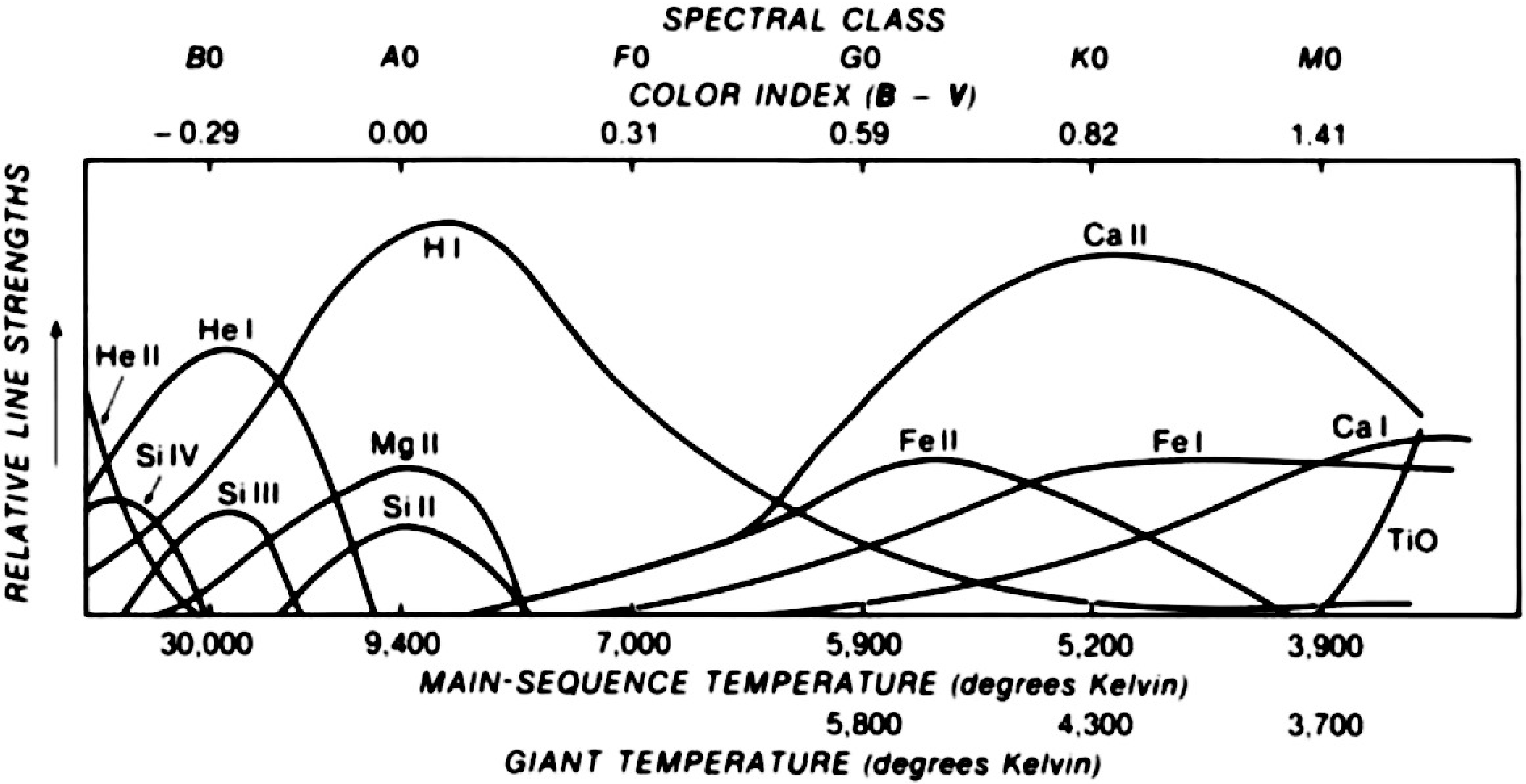

Roman number indicate the ionization stage of the atoms: e.g., H I means neutral hydrogen, He II corresponds to He^{+}, Si III to SI^{++} etc.

Type	Colour	Approximate Surface Temperature	Main Characteristics	Examples
O	Blue	$>$ 25,000 K	Singly ionized helium lines either in emission or absorption. Strong ultraviolet continuum.	10 Lacertra
B	Blue	11,000 - 25,000	Neutral helium lines in absorption.	Rigel Spica
A	Blue	7,500 - 11,000	Hydrogen lines at maximum strength for A0 stars, decreasing thereafter.	Sirius Vega
F	Blue to White	6,000 - 7,500	Metallic lines become noticeable.	Canopus, Procyon
G	White to Yellow	5,000 - 6,000	Solar-type spectra. Absorption lines of neutral metallic atoms and ions (e.g. once-ionized calcium) grow in strength.	Sun, Capella
K	Orange to Red	3,500 - 5,000	Metallic lines dominate. Weak blue continuum.	Arcturus, Aldebaran
M	Red	$<$ 3,500	Molecular bands of titanium oxide noticeable.	Betelgeuse, Antares

2.3 Stellar luminosities and Hertzsprung-Russel-Diagram

A direct estimate of the luminosity of a star requires the knowledge of its distance: $\mathbf{M} = \mathbf{m} - \mathbf{5}\log\left(\frac{\mathbf{D}}{\mathbf{10pc}}\right)$. Distance determination was and to some degree still is one of the basic problems in astrophysics. For nearby stars, the distances can be measured with parallaxes:

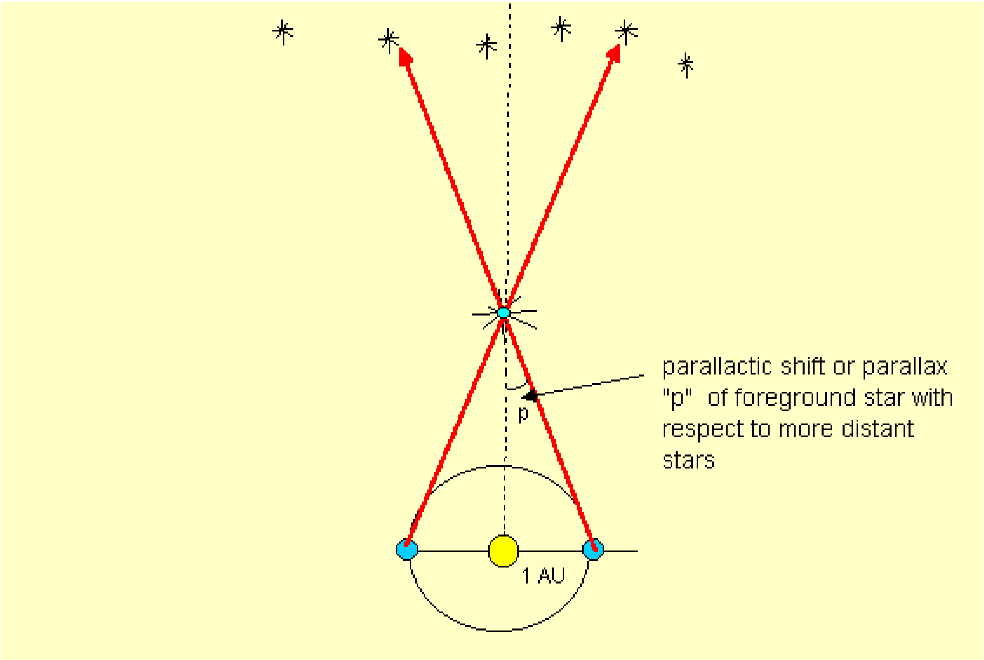

$$\frac{1AU}{d_*} = p$$

With ground based observations distances up to 10 pc can me measured with about 10% accuracy, the Hipparcos-satellite derived distances up to 1kpc (in orbit there are no disturbing effects of the earth's atmosphere like seeing and deflection!).

Once one knows the distances and hence the absolute magnitudes, one can plot **the fundamental diagram of stellar astrophysics:**

the **color-magnitude diagram** or **Hertzsprung-Russel** diagram.

Already around 1910, Rosenberg, Hertzsprung and Russel discuss what is now called the Hertsprung-Russel Diagram. The name Hertzsprung-Russel diagram is reserved for a diagram which shows luminosity as a function of effective surface temperature of stars. However, the Hertzsprung-Russell diagram is (almost) uniquely linked to the observationally easier to obtain color-magnitude diagram because most colors vary monotonically as a function of stellar surface temperature.

Colour-magnitute diagrams are an important tool in astrophysics with regard to stellar evolution and age- and metallicity determinations of star clusters (see below).

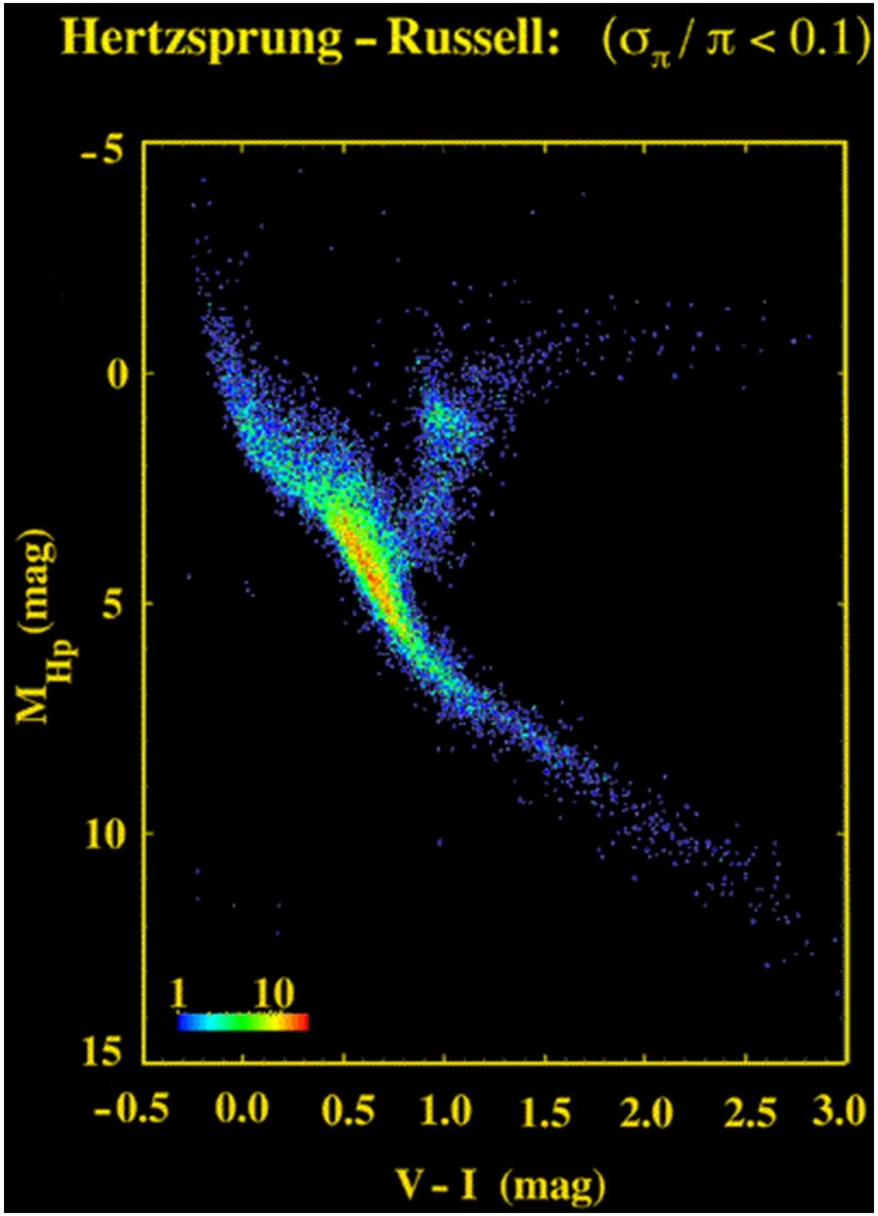

The color-magnitude diagram of all Hipparcos stars with relative distance error < 0.1.

The Hertzsprung-Russell diagram shows that at a given effective temperature (or color) stars with different luminosities do exist. Therefore, the Harvard classification was supplemented by **luminosity classes** in the Yerkes (or Morgan-Keenan) scheme:

Ia	Most luminous supergiants
Ib	Less luminous supergiants
II	Luminous giants
III	Normal giants (giant branch)
IV	Subgiants
V	Main sequence stars (dwarfs) 90% of all stars
VI	sub dwarfs
W.D.	white dwarfs

In the complete Harvard-Yerkes Morgan-Keenan classification a star is defined by three quantities: **spectral class, sub class, luminosity class**. The sun and Vega are main sequence stars of type G2V and A0V, respectively; Arcturus is a red giant of type K0III, and Deneb is a A0Ia supergiant. The physics behind the different luminosity classes is explained below.

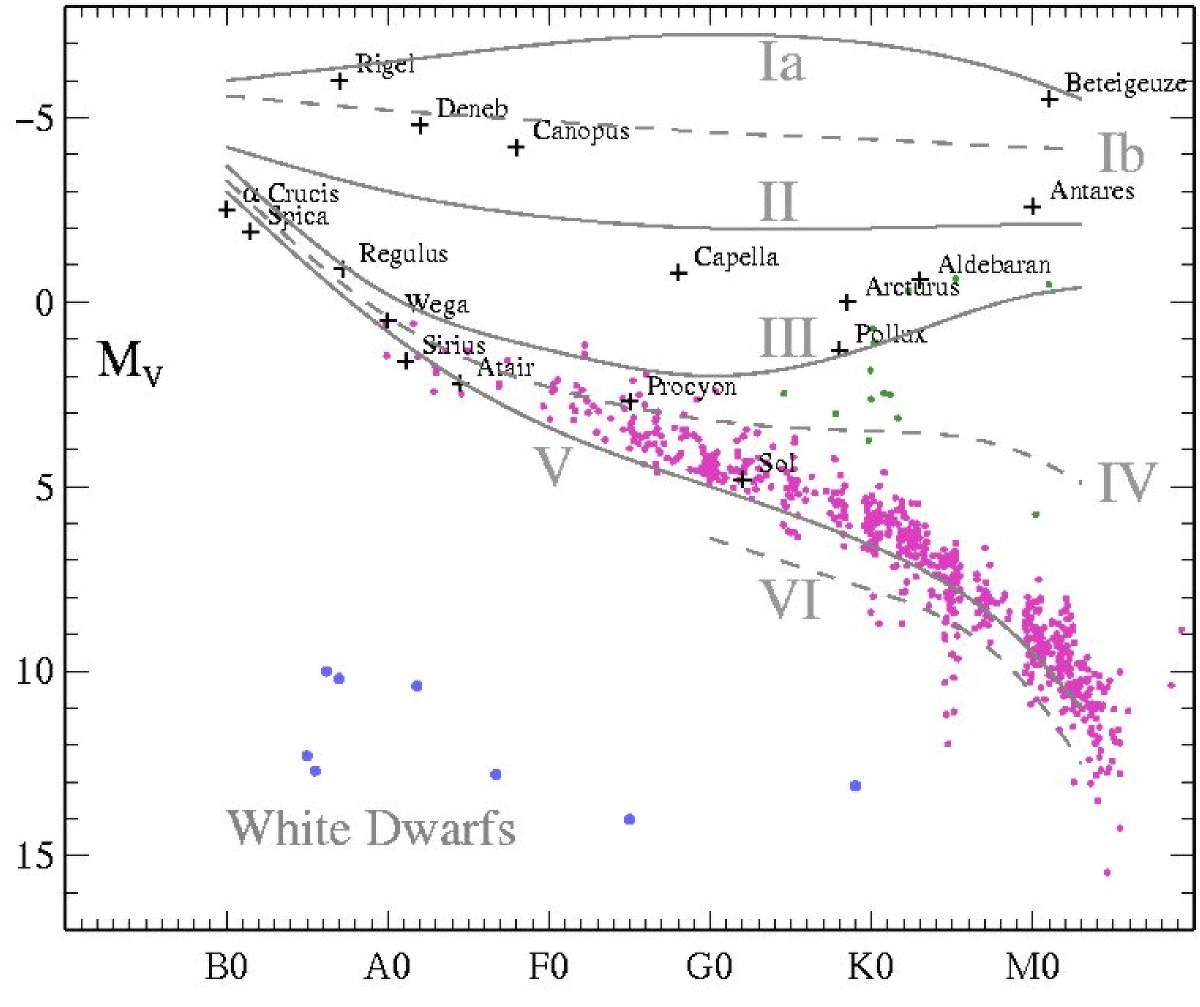

Luminosity classes in the Hertzsprung-Russel-Diagram.

The luminosity of a star is related to the stellar radius R and effective temperature T_{eff} via:

$$L = 4\pi\, R^2\, \sigma_B T_{eff}^4$$

Therefore a higher luminosity for the same spectral class (and therefore the same T_{eff}) implies a larger radius. This implies a smaller gravitational acceleration on the surface of the star and thus a smaller pressure in the region of line formation. This affects both the strengths and the widths of absorption lines (pressure broadening, see chapter 1).

Consequently, giants, main sequence stars and white dwarfs can be distinguished by an analysis of their spectra. **A detailed spectral analysis can yield the effective temperature of a star very accurately, and rough estimates of its intrinsic luminosity, radius and distance.**

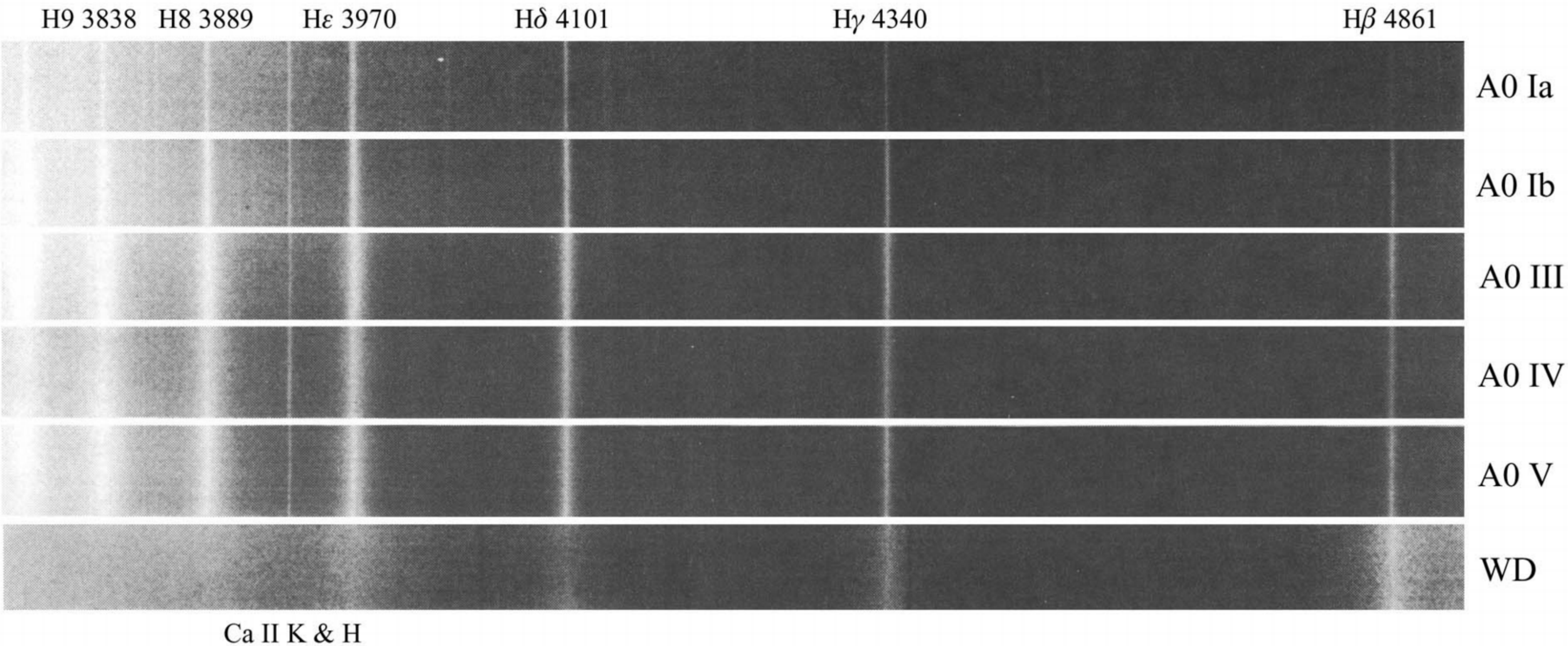
H9 3838
H8 3889
Hε 3970
Hδ 4101
Hγ 4340
Hβ 4861
A0 Ia
A0 Ib
A0 III
A0 IV
A0 V
WD
Ca II K & H

2.4 Interpretation of stellar spectra

The spectra of stars contain information about the physical conditions in the stellar atmosphere and allow to derive:

- **effective temperature** T_{eff}
- **gravitational acceleration** $g = G\frac{M}{R^2}$
- **luminosity** L
- **chemical composition**

More quantitatively, based on the Saha- and Bolzmann–equation we have the following dependencies:

- relative ionisation states depend on T_{eff} and n_e.
- relative population numbers at given ionisation state depend only on temperature.
- absolute population numbers depend on the chemical abundance of an element, on T_{eff}, n_e and ρ or g (gravitational acceleration in the stellar photosphere).

- absorption line shapes depend on the temperature (line core) and pressure P (line wings) in the atmosphere and, in turn, also depend on the density n.

The relation between g, ρ and T can be understood using the barometric formula of hydrostatic stability of the atmosphere:

$$\frac{dp}{dr} = -\rho\, g \quad \text{and} \quad \frac{dp}{dr} \approx \frac{kT}{\mu m_p}\frac{d\rho}{dr} \qquad (T \approx const.)$$

or:

$$\frac{d\rho}{dr} = -\frac{\rho}{H} \qquad \text{with} \quad H = \frac{kT}{g\mu m_p} \qquad (H \approx 300\text{km for the sun})$$

Furthermore we have:

$$d\tau_\lambda = -\kappa_\lambda dr \quad \text{and} \quad \kappa_\lambda \approx \rho f_{o,\lambda}$$

wher $f_{o,\lambda}$ is called oscillator strengths and is derived from atomic physics, Saha and Boltzmann formulae). It follows:

$$\frac{d\rho}{d\tau} = \frac{\rho}{H}\frac{1}{\rho f_{o,\lambda}}$$

which is readily integrated because $H =$const. and $f_{o,\lambda} \approx$const.:

$$\rho(\tau) \approx \frac{\tau}{H f_{o,\lambda}}$$

or:

$$\rho(\tau = 1) \approx \frac{g\mu m_p}{kT}\frac{1}{f_{o,\lambda}}$$

Example: Using the Saha and Boltzmann formulae, how can we understand the **variation of the Balmer line strengths along the Harvard sequence?**

- As the excitation occurs from the $n = 2$ state, the temperature has to be high enough to populate this level. This is the case for most of the stars.
- The $n = 2$ level will become more and more populated if we pass from K stars to A stars, as with rising temperature because of Boltzmann: exp$[-E(Ly_\alpha)/kT]$ is rising. $\rightarrow$ Hydrogen lines get stronger.
- For very high temperatures (stars hotter than A) the neutral H-atoms are ionised instead of being excited to the $n = 2$ level (Saha-equation). Although n_2/n_1 is still increasing, the absolute number of n_2 is decreasing, as more and more hydrogen atoms loose their electrons. $\rightarrow$ Hydrogen lines get weaker.

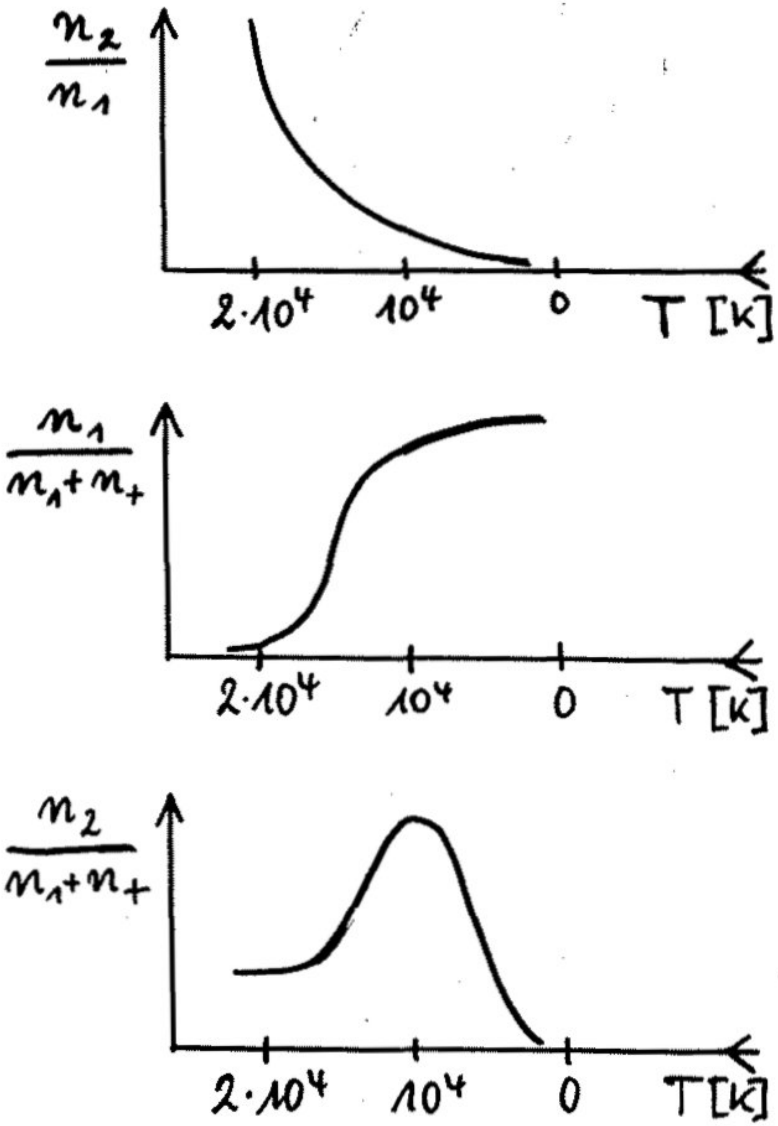

n_2	=	H atoms in $n = 2$ level
n_1	=	H atoms in $n = 1$ level
n_+	=	H ions (protons)

All other lines behave analogously to the Balmer lines, depending on the temperature.

A key tool to determine the abundances in stellar atmospheres is the **equivalent width** w, defined via:

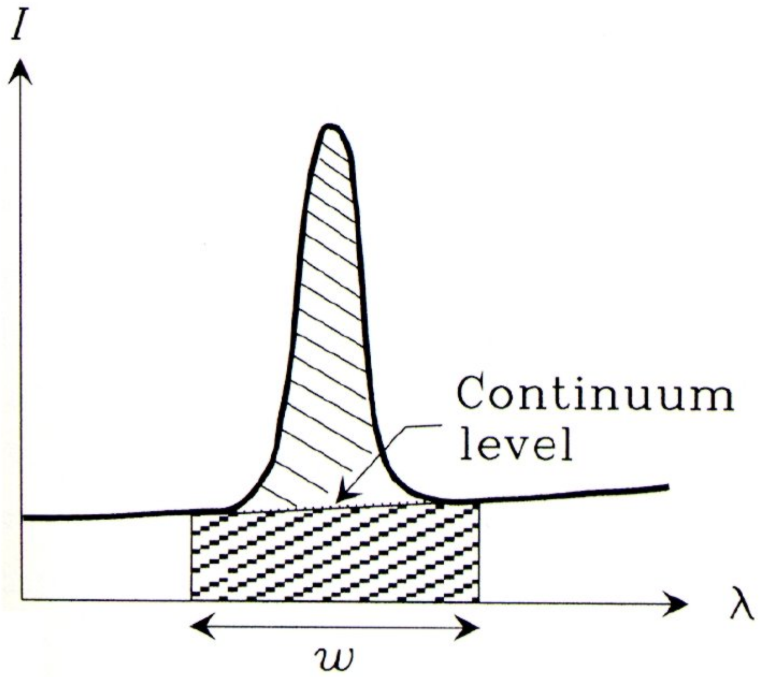

$$w = \int_{line} R_\lambda d\lambda = \int_{line} \frac{I_{\mathrm{cont}} - I_\lambda}{I_{\mathrm{cont}}} d\lambda$$

The equivalent width w evidently has the unit of a wavelength. Geometrically, the product of continuum flux times equivalent width covers the same area in a spectrum as the absorption or emission line does.

The equivalent width increases with increasing number of ions in the corresponding quantum state. In the optically thin case, the increase is linear. For higher densities of ions, the absorption line starts to saturate and the equivalent width almost stops increasing (at which density this happens depends on the Doppler broadening). Then, at very high densities, the damping wings from the Lorentzian profile starts to show and the equivalent width grows again, but only with the square root of the number of the ions. The curve which decsribes this behaviour is called **curve of growth** (shown below for different Doppler broadening).

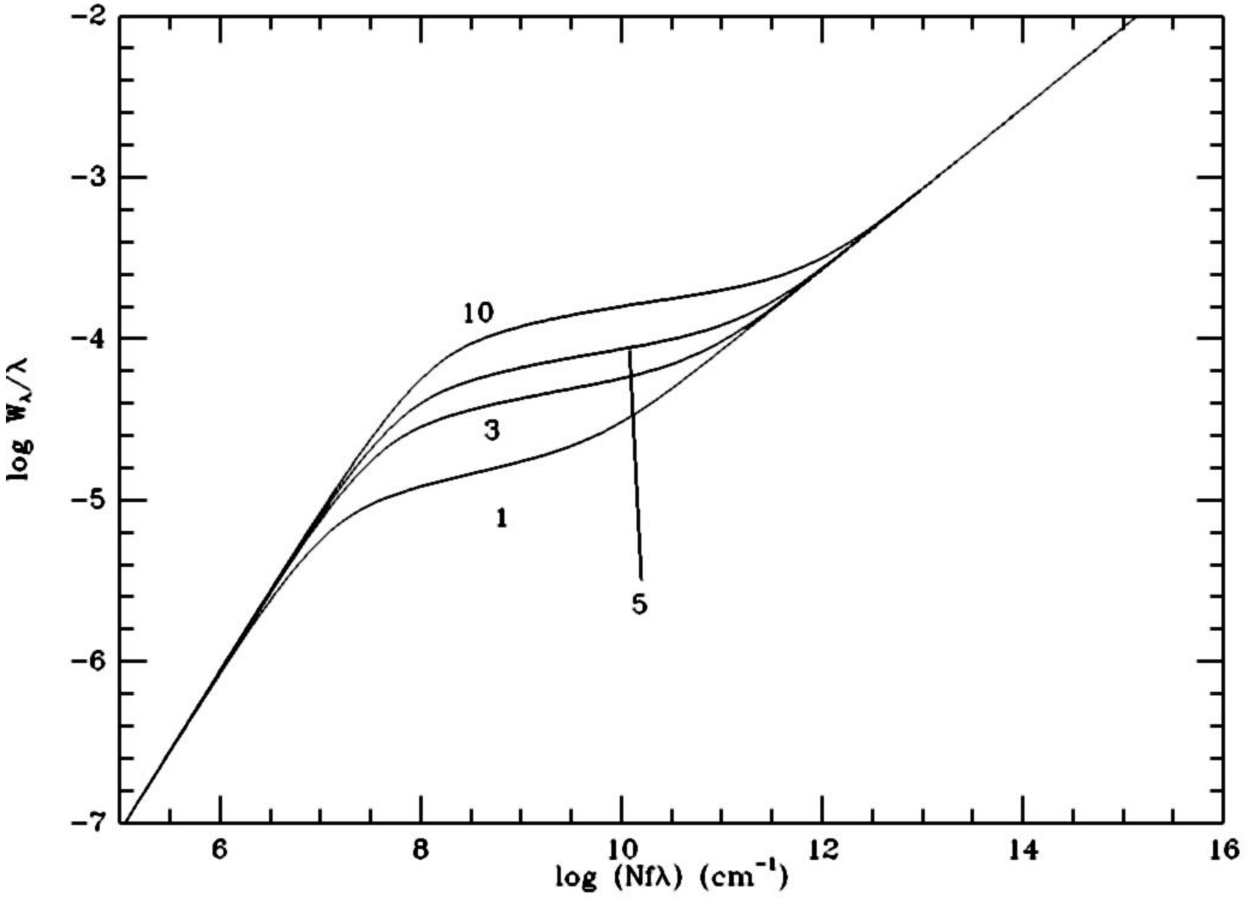

Besides the shapes and equivalent widths of lines, breaks in the spectra can also be indicative of fundamental parameters. The so-called **Balmer-break** D_B at 3646Å is an excellent temperature indicator for hot stars with a maximum around $T = 10000$K. D_B varies in accordance with the hydrogen lines but is easier to measure, especially for very faint objects.

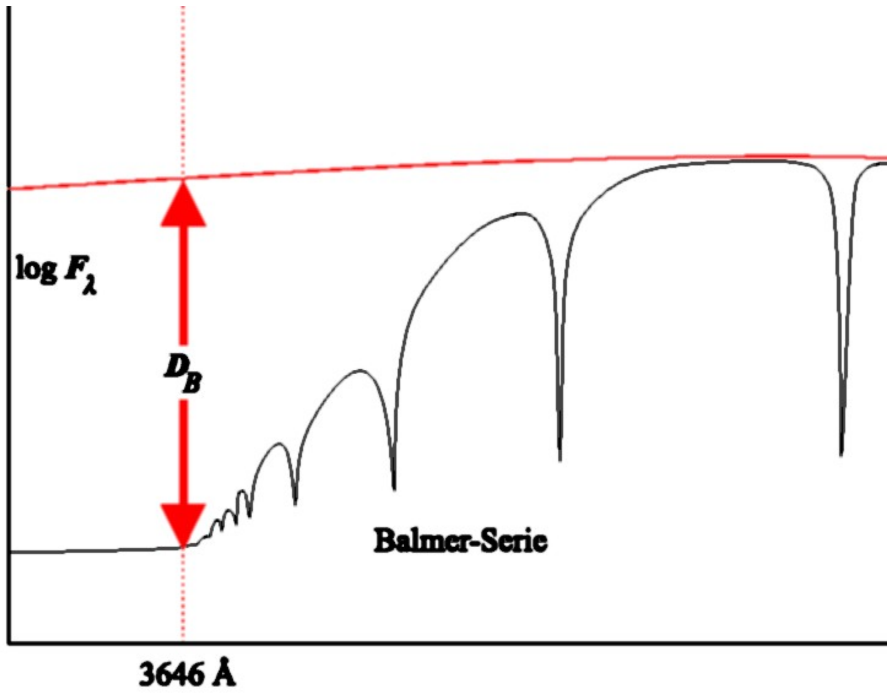

2.5 The solar surface

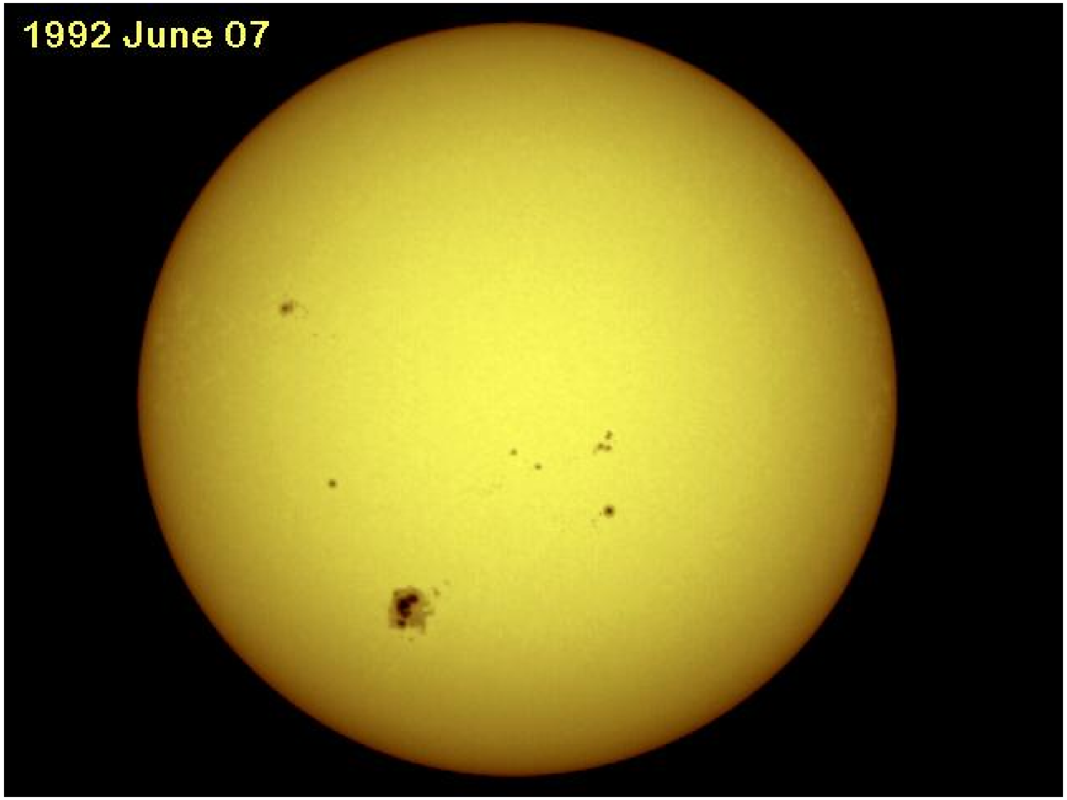

Solar photosphere:

- thin shell: $\frac{\Delta R}{R} \sim 10^{-3}$
- Temperature: $T \sim 5800\ K$ (Sunspots $\sim$ 4800 K)
- produces visible light
- produces absorption spectrum

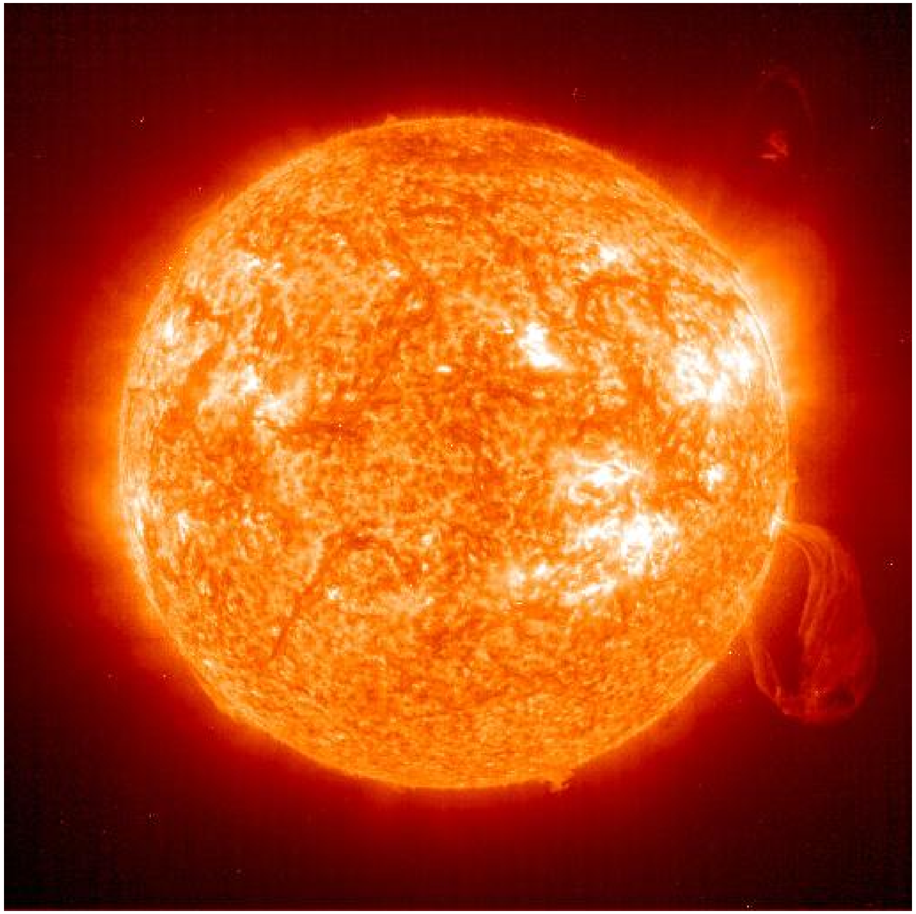

Solar Corona:

- thin, outer atmosphere
- produces EUV emission and X-rays
- Temperature: $T \sim 1.5 \times 10^6$ K
- Magnetic flares and prominences heat corona, drive solar wind and are origin of high energy particles
- Granulation is due to convection in photosphere
- picture in EUV by Solar and Heliospheric Observatory

Corona during the Total Solar Eclipse of 1999 Aug 11 (Lake Hazar, Turkey) with helmet streamers (solar plasma trapped by the Sun's magnetic field, $T \sim 10^6$ K)

Solar Cycle:

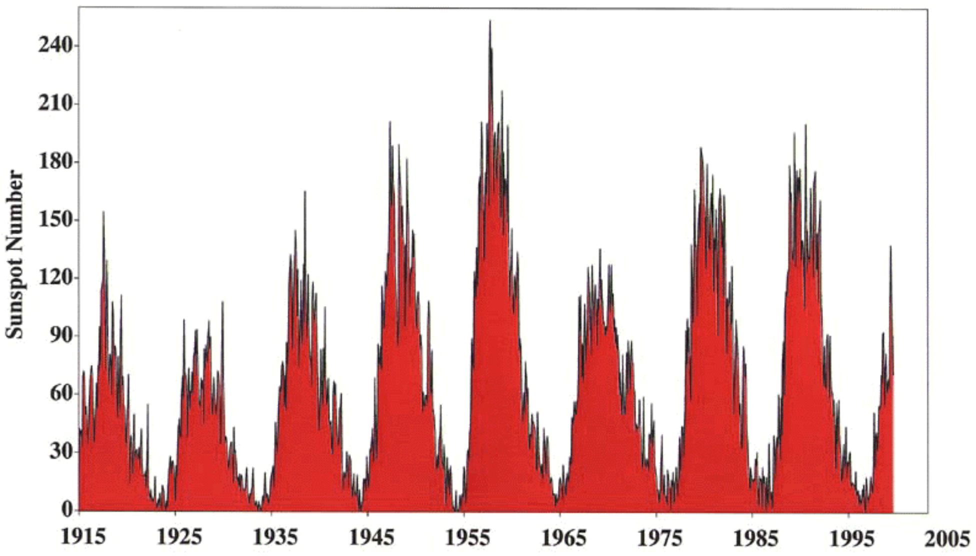

- Number of sunspots increases and decreases every 11 years
- Next maximum will occur in about 2002
- Sunspots are connected to magnetic activity of the sun
- Polarisation of magnetic field changes every 22 years

Schematic structure of the Sun:

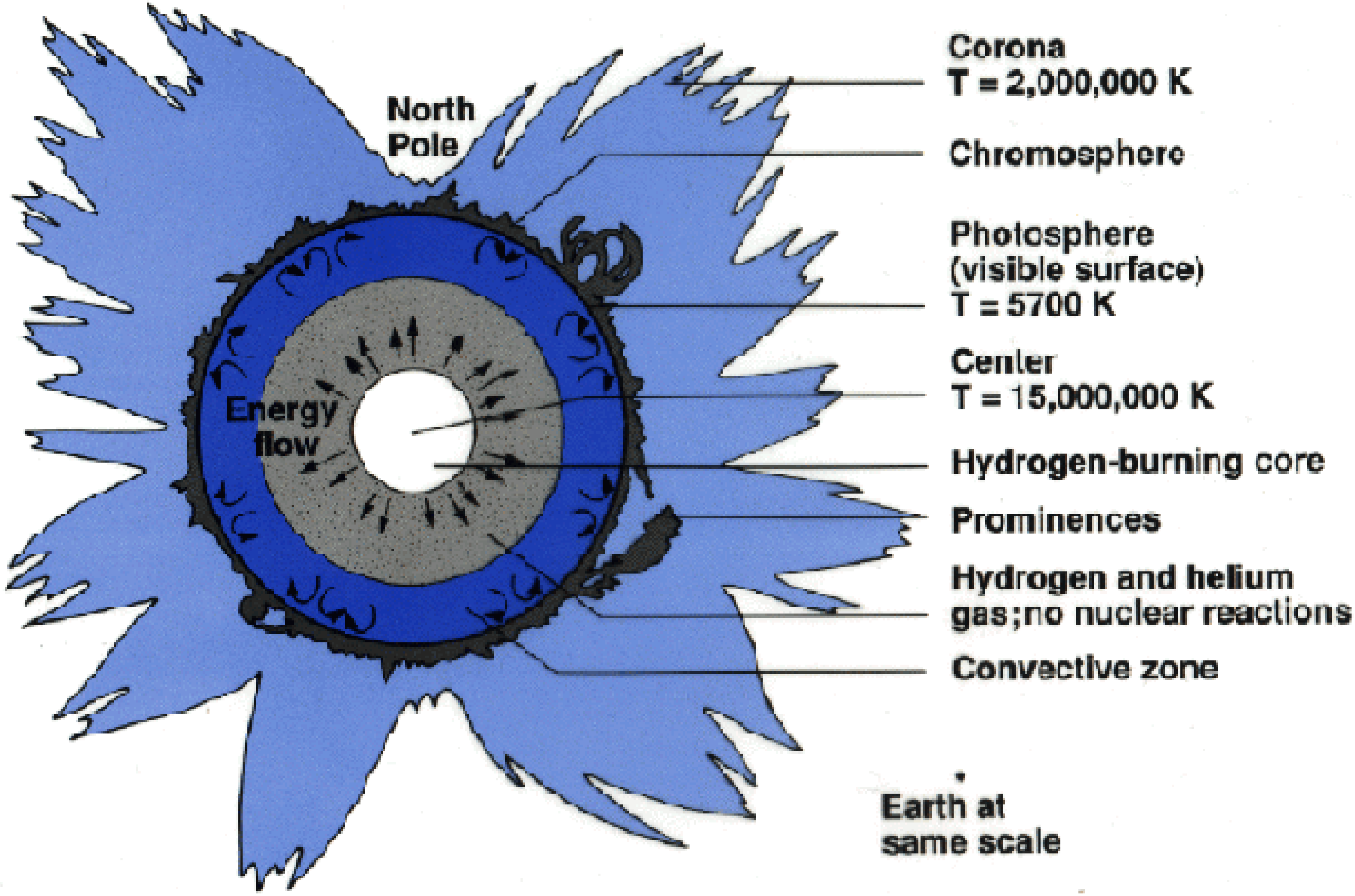

2.6 Fundamental properties of stars

Five fundamental parameters characterize stars:

luminosity, temperature, mass, radius and chemical abundance.

Up to now, we have discussed the determination of effective temperatures, luminosities and abundances in stellar atmospheres. To check the validity of stellar models it is crucial to also directly determine stellar radii and stellar masses, as these allow to check the relation between luminosities and effective temperatures of stars.

2.6.1 Stellar radii

Direct measurments of stellar radii have up to now been only possible for a very small number of stars. The reasons are:

- resolution of telescopes is limited by

$$\varphi = 1.2\,\frac{\lambda}{D} \approx 0''.1\;\frac{\lambda/400nm}{D/1m}$$

- atmospheric turbulence and small differences in the diffraction index of air induce a broadening of point sources to:

$$\varphi_{seeing} = 0''.5 \ldots 1''.$$

for a typical observatory on a mountain. This is called **atmospheric seeing**.

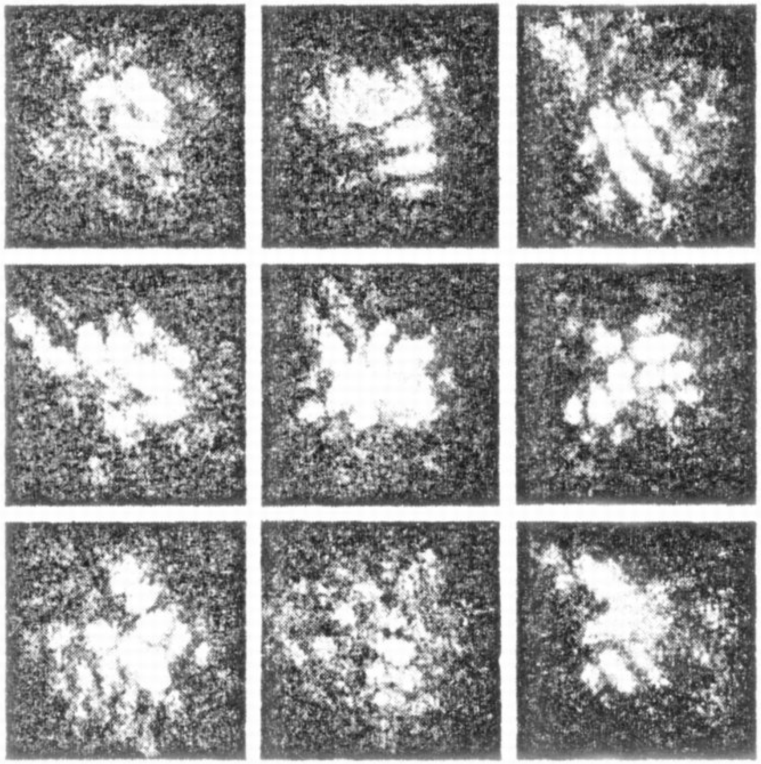

Short exposures (~ 0.1 s) which come close to the typical fluctuation time scale in the earth' atmosphere, reveal the structure of the **seeing**. The regular seeing disk with a diameter of about 0.5" to 1" separates into individual **speckles**. The number of the speckles corresponds to the number of turbulence cells above the telescope. The speckles have an angular size similar to the diffraction limit of the telescope.

For comparison, the sun seen from only 1 pc distance would have an angular diameter of $\varphi_{\odot,1pc} \approx 0''.01$ and, therefore, appears as a point source.

Radii from eclipsing binaries

A technically much easier method to determine stellar radii uses eclipsing binaries. Fortunately, most stars live in binary systems and so at least some binaries are eclipsing.

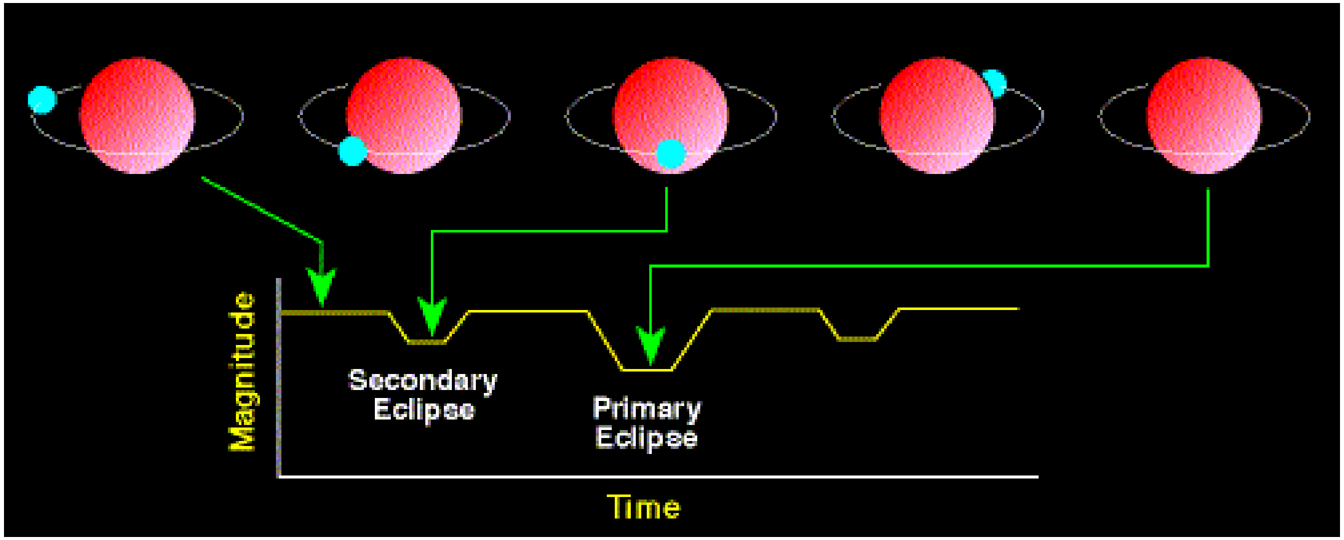

Assume that at t_1 the eclipse starts (the stars touch in projection), between t_2 and t_3 the eclipse is complete, and at t_4 the eclipse ends. For the primary eclipse, let $R_2 < R_1$. We then have:

$$\frac{t_4 - t_1}{T} = \frac{2R_1 + 2R_2}{l} \tag{2.1}$$

$$\frac{t_3 - t_2}{T} = \frac{2R_1 - 2R_2}{l} \tag{2.2}$$

with l being the length of the orbit from star 2 around star 1, and T being the orbital period.

Assuming a circular orbit, the orbit's velocity is constant and may be measured from the maximal Doppler shift of the spectral lines. As T is known from the light curve it is possible to determine l:

$$l = vT$$

From (1) and (2) follow the radii R_1 and R_2 without knowing the distance of the star. If the maximal angular separation may be observed, then the absolute separation of the two stars can be calculated. Analogous, if T_{eff} is known, the distance follows from $L = 4\pi R^2 \sigma T_{eff}^4$ and the observed flux.

Radii from interferometry

Interferometry can be used to resolve stars despite of seeing and insufficient optical quality.

Imagine a telescope of which the aperture is completely covered except for 2 pinholes. A point source generates an interference pattern with

- Maxima at $\varphi_{ma,n} = n\frac{\lambda}{D_0}$
- Minima at $\varphi_{ma,n} = (n + 1/2)\frac{\lambda}{D_0}$

where D_0 ist the separation of the two pinholes and $n = 0, \pm 1, \pm 2, ...$ A second point source located in angular distance γ generates a similar pattern, but shifted by angle γ. Its maxima are located at $\tilde{\varphi} = \varphi - \gamma$.

If D_0 is small, the separation between 0. and 1. maximum: $\Delta\varphi = \varphi_{ma,0} - \varphi_{ma,1}$ is larger than γ and both pattern overlap $(\Delta\varphi >> 0)$.

By increasing D_0, $\Delta\varphi$ decreases and for $\gamma = \lambda/(2D_0)$ the 0. maximum of the second point source is located at the 1.minimum of the first source: $\rightarrow$ the interference pattern disappears.

$\rightarrow$ Disappearence of the interference pattern gives the angular separation of the sources :

$$\gamma = \lambda/2D_0$$

For a disk-like object the same considerations yield to a similar result: A disk behaves like two point sources, which are separated 0.41 times the diameter of the disk.

Therefore it is possible to resolve the disk of a star if $0.41\gamma = \lambda/2D_0$.

$$\gamma = 1.22\,\frac{\lambda}{D_0}$$

This is the same as for the ordinary telescope, BUT because of the larger extend of the interference pattern it is much less sensitive against seeing so that this method works up to the resolution of the telescope.

With 2 or more telescopes (ESO VLT: 4$\times$8m, separated up to 200m) it is possible to achieve very high angular resolution. First successes have been achieved at Keck and VLT.

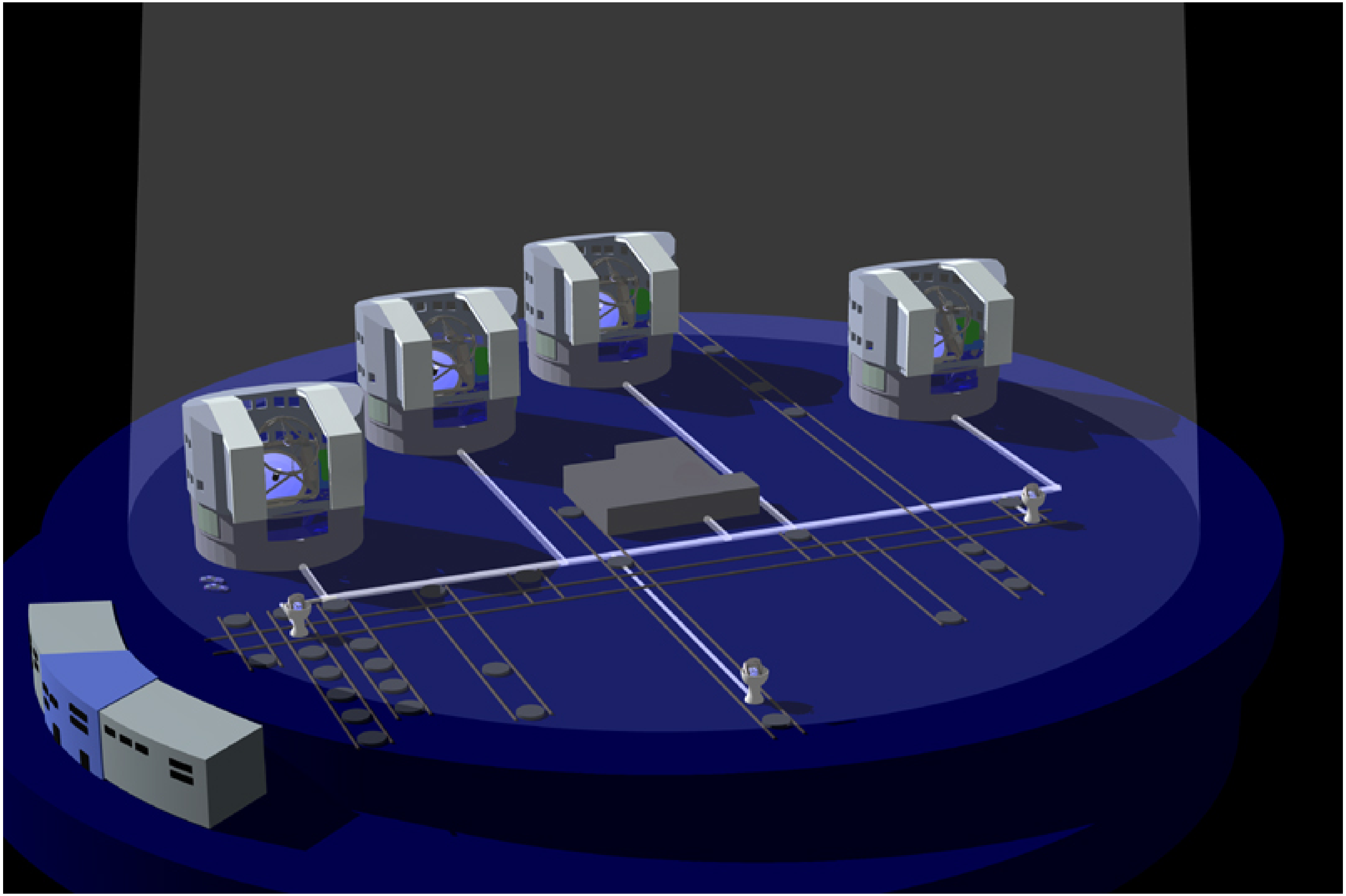

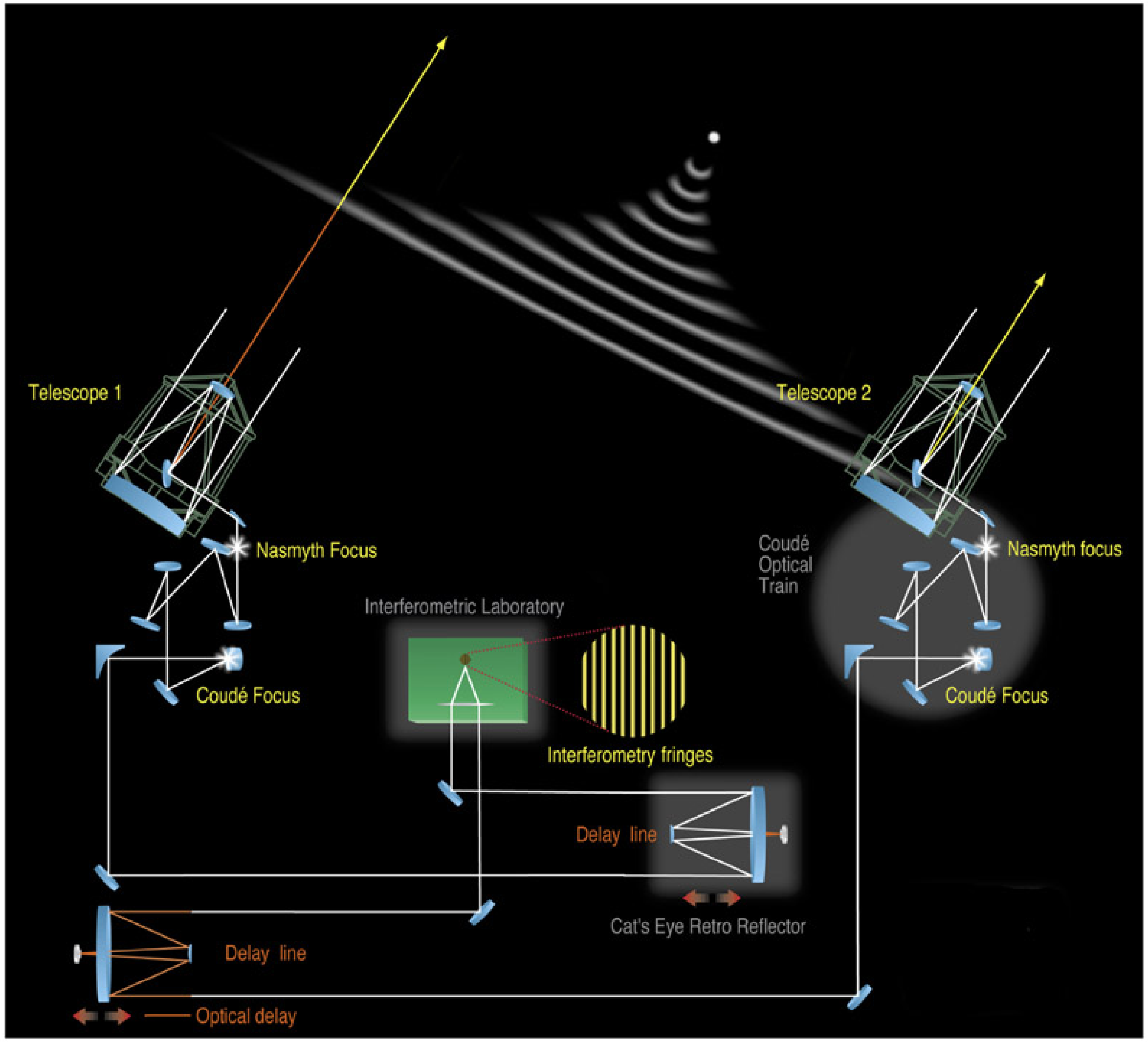

Overview of the VLT Interferometer

ESO PR Photo 10c/01 (18 March 2001)

© European Southern Observatory

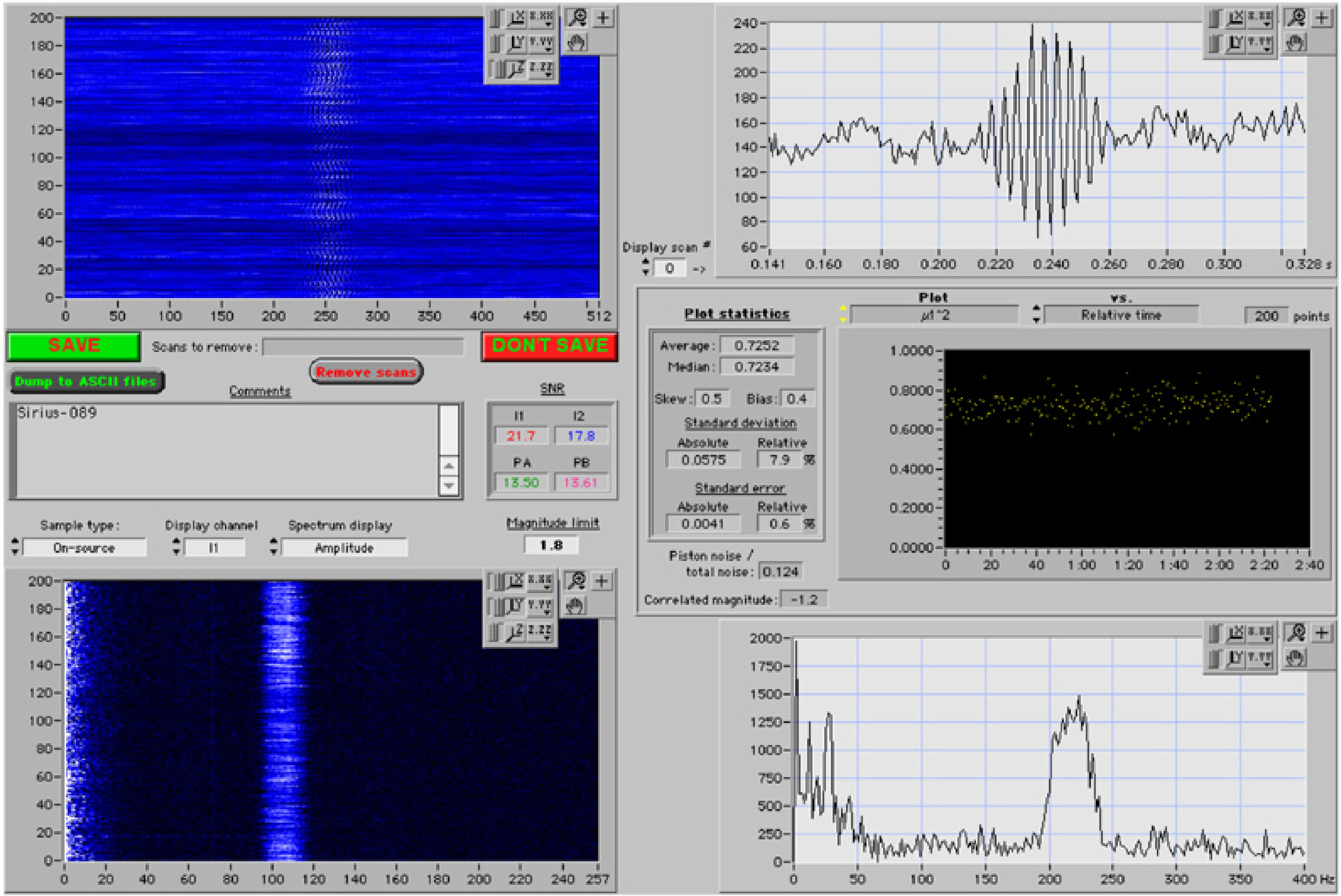

'First Fringes' from Sirius with VLTI

ESO PR Photo 10a/01 (18 March 2001)

© European Southern Observatory

Measured stellar radii

Type	T_{eff}	$R/R_{\odot}$	
M5V	3100	0.3	
M0V	3800	0.6	
G0V	6000	1.1	main sequence:
A0V	10000	2.6	R increases with T_{eff}
B0V	30000	7	
O5V	45000	18	
M0Ia	3700	500	
G0Ia	5800	200	giants:
A0Ia	9400	100	R decreases with T_{eff}
B0Ia	27000	30	
O5Ia	40000	25	

white dwarfs: $R \approx 1/100 R_{\odot}$ independent of T_{eff}.

2.6.2 Stellar Masses

As stellar radii, stellar masses can be determined indirectly from spectral analysis. If the radius R is known it is possible to obtain the mass from $g = \frac{GM}{r^2}$. As g can roughly be determined from spectral ananlysis only within a factor of 2, the masses have the same error. A better method uses visual binaries:

Up to now around 100 binaries are observed, for which orbital inclination and shape are known simultaneously. The motion of the two stars is determined using the Kepler–law.

- If the distance is known and the apparent motions of *both* components is observable, the total mass follows from Kepler's third law:

  $$M_1 + M_2 = \frac{4\pi^2}{G}\frac{a^3}{T^2} \qquad \text{with } a = a_1 + a_2,$$

  using the center-of-mass:

  $$a_1 M_1 = a_2 M_2$$

  we get the individual masses M_1 and M_2.

- If only the orbit of one star is known (for large mass ratio of the 2 stars), we can still determine the total mass.

Stellar masses from eclipsing binaries

In case of circular orbits:

- eclipse: $\longrightarrow \frac{R_1}{l}, \frac{R_2}{l}, T$
- Doppler shift: $\rightarrow \frac{v}{c} = \frac{\Delta\lambda_{max}}{2c}$

we obtain:

$$a_{1/2} = v_{1/2}\frac{T}{2\pi}$$

and

$$M_1 + M_2 = \frac{4\pi^2}{G}\frac{a^3}{T^2} \qquad \text{with} \qquad a = a_1 + a_2, \quad a_1 M_1 = a_2 M_2$$

$\rightarrow$ we can derive: M_1, M_2, R_1, R_2.

In the case of elliptical orbits the situation is more complicated, but essential parameters can still be determined from the Doppler profiles.

2.6.3 Mass-Radius-Luminosity relations for the main sequence

This covers 90% of all stars.

- Mass–luminosity relation ($0.1 M_\odot < M < 100 M_\odot$):

$$L \propto M^4 \qquad \text{for} \quad M > 0.6 M_\odot$$
$$L \propto M^2 \qquad \text{for} \quad M < 0.6 M_\odot$$

- Mass–radius relation:

$$R \propto M^{0.6} \qquad \text{for} M > 0.6 M_\odot$$

- Luminosity–temperature relation:

$$L \propto T_{eff}^7$$

- Gravity

$$g \approx const \approx g_\odot$$

Mass–luminosity relation for the main sequence

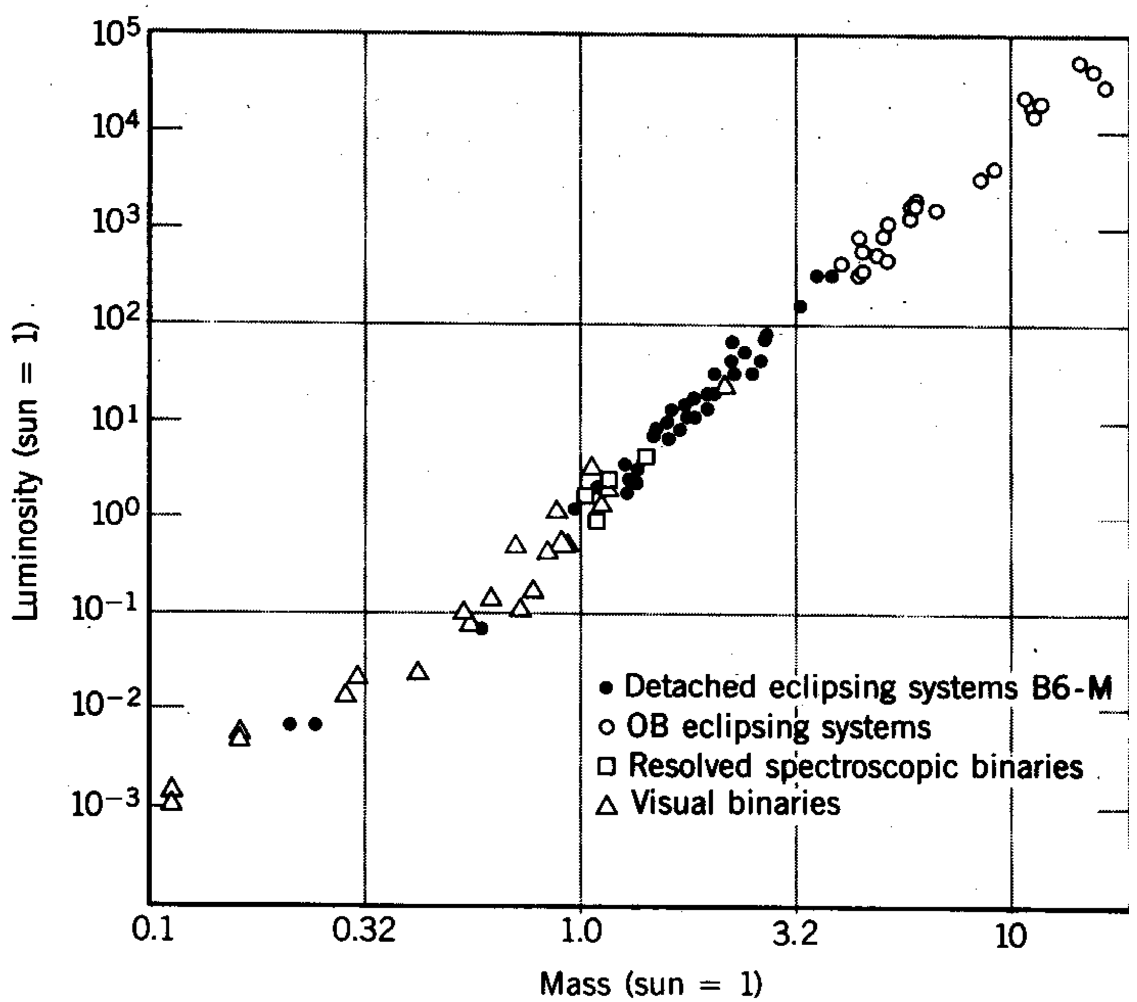

The mass – luminosity relation for stars, as determined from binary systems, in which the individual masses can be found.

2.6.4 Mass–radius–relation for white dwarfs

- white dwarfs have a very narrow mass distribution:

$$M_{WD} \approx 0.6 \pm 0.2 M_\odot$$

  some have masses up to $M > 1.4 M_\odot$, none masses above.

- the mass–radius relation is

$$R \propto M^{-1/3}$$

- the radius is not a function of T_{eff}

$\rightarrow$ White Dwarfs are distinct from ordinary main sequence stars. The theory of stellar structure explains this by pressure support through a degenerate electron gas (see below).

2.6.5 Chemical abundances of stars

The sun is typical for disk stars in the Milky Way. The sun's composition by mass is: 72% Hydrogen, 26% Helium, 2% all heavier elements (mostly C, O). This is the atmospheric and original composition, i.e. before nuclear burning sets in.

The metal poor halo stars of the Milky Way have up to a factor 1000 lower abundances in heavy elements, the bulge stars can have up to 5 times higher abundance.

We will discuss abundances further below.

2.6.6 Main Solar Parameters

- Distance Sun $\mapsto$ Earth: 1 AU = 1.5×10^8 km = 8.3 light-minutes
  (Earth $\mapsto$ Moon = 1.3 light-sec)
- Diameter: $D_\odot = 1.4 \times 10^6\ km = 5\ \mathrm{light-sec} = 100 \times D_{Earth}$
- Mass: $M_\odot = 2 \times 10^{30} kg = \frac{1}{3} \times 10^6 M_{Earth}$
- Density: $< \rho >= 1.4\ \frac{g}{cm^3}$ (slightly more than water);
  Central: $\rho_c = 150\ \frac{g}{cm^3}$;
  Photosphere: $\rho_{photo} = 3.5 \times 10^{-7} \frac{g}{cm^3} = \frac{1}{3000}\ \rho_{air}$
- Temperature:
  Central: $T_c = 1.5 \times 10^7$ K; Photosphere: 5800 K; Sunspots: 4800 K;
  Corona: $10^6 - 10^7$ K
- Composition (by mass): 72% Hydrogen, 26% Helium, 2% all other elements
- Rotation period: 25 days (equator); 28 days (higher latitudes); 31 days (polar)
- Luminosity: $L_\odot = 3.85 \times 10^{33} erg/s$